Using Well-Understood Single-Objective Functions in Multiobjective Black-Box Optimization Test Suites

Dimo Brockhoff dimo.brockhoff@inria.fr
Inria, research centre Saclay and
CMAP UMR 7641 École Polytechnique CNRS, France

Tea Tušar tea.tusar@ijs.si
Jožef Stefan Institute, Ljubljana, Slovenia

Anne Auger anne.auger@inria.fr
Inria, research centre Saclay and
CMAP UMR 7641 École Polytechnique CNRS, France

Nikolaus Hansen nikolaus.hansen@inria.fr
Inria, research centre Saclay and
CMAP UMR 7641 École Polytechnique CNRS, France

Abstract

Several test function suites are being used for numerical benchmarking of multiobjective optimization algorithms. While they have some desirable properties, like well-understood Pareto sets and Pareto fronts of various shapes, most of the currently used functions possess characteristics that are arguably under-represented in real-world problems. They mainly stem from the easier construction of such functions and result in improbable properties such as separability, optima located exactly at the boundary constraints, and the existence of variables that solely control the distance between a solution and the Pareto front. Here, we propose an alternative way to constructing multiobjective problems—by combining existing single-objective problems from the literature. We describe in particular the `bbob-biobj` test suite with 55 bi-objective functions in continuous domain, and its extended version with 92 bi-objective functions (`bbob-biobj-ext`). Both test suites have been implemented in the COCO platform for black-box optimization benchmarking. Finally, we recommend a general procedure for creating test suites for an arbitrary number of objectives. Besides providing the formal function definitions and presenting their (known) properties, this paper also aims at giving the rationale behind our approach in terms of groups of functions with similar properties, objective space normalization, and problem instances. The latter allows us to easily compare the performance of deterministic and stochastic solvers, which is an often overlooked issue in benchmarking.

Keywords

Black-box optimization benchmarking, multiobjective optimization, algorithm comparison, benchmark suite generator.

1 Introduction

Numerical benchmarking is an important part of (black-box) optimization that helps to understand algorithm behavior and recommend algorithms. In order to obtain mean-

ingful results, a benchmarking experiment should be (i) based on a thorough, well-documented and well-understood methodology and (ii) either be conducted on real-world problems of interest or a collection of artificial test functions that possess comprehensible difficulties observed in practical optimization problems. This holds true for both single- and multiobjective problems but for the latter, the methodology is less advanced at the moment.

Many artificial test functions that are frequently used in multiobjective optimization have been derived by setting up the Pareto front shape first without relating it to the intrinsic difficulties of the objective functions. Such an approach has the advantage that the analytical forms of the Pareto front and the Pareto set can be exploited to facilitate the performance assessment. Another aspect of state-of-the-art test suites for multiobjective optimization is the fact that not much progress has been made to avoid the overrepresentation of functions that are too simple or have questionable properties. Several existing (and still frequently used) multiobjective test suites, for example, contain a large share of functions that are separable, have the Pareto set on the domain boundary, or contain distance and position variables [1] —artificial features not reflecting well the difficult black-box problems observed in practice.

The most complete reference for multiobjective test function suites is the work of Huband et al. (2006). The authors not only review all available test suites at the time of writing (not many new have been introduced thereafter), but also give general advice on the desired properties of multiobjective test functions. Based on these recommendations, Huband et al. finally propose a generic test function generator and use it to create the WFG function suite with nine scalable test functions. These test functions, however, are constructed in a similar manner as the above mentioned suites with the shape of the Pareto front being the first design criterion. After that, transformations in the search and objective space give the functions some desired properties, like non-separability and multimodality.

In the context of single-objective algorithm benchmarking, a lot of progress has been made in recent years in the design of artificial test functions that represent a wide range of difficulties observed in practice. The black-box optimization benchmarking test suite (`bbob`, Hansen et al. (2009)) in particular has received wide acceptance as its 24 test functions have various advantages over previous test suites. The functions are well understood and expose algorithms to a variety of real-world difficulties such as multimodality, ill-conditioning, non-separability of the variables, and non-linearities. The `bbob` functions are grouped into five function groups with functions within a group sharing similar difficulties (such as multimodality with weak global structure) and with the aim to not overemphasize certain difficulties. Each function has one or several concrete scientific questions associated with it that can be answered by looking at algorithm performance results on that function (or in combination with another function). General statements beyond the tested concrete functions are possible by testing invariance properties of algorithms such as scaling, rotation and affine invariance. The `bbob` functions also come in the form of instances which allows us to easily compare deterministic and stochastic algorithms (see Section 4.4).

In contrast to the previously mentioned approaches to building multiobjective test suites, we suggest to focus on introducing the known difficulties of real-world prob-

[1] A function is said to have a *distance variable* if changing this variable only results in dominating or dominated solutions. In other words, a distance variable determines solely the distance of a solution from the Pareto front. A *position variable*, in turn, only results in incomparable solutions when changed (see Huband et al. (2006) for details).

lems into the test suite. This is analogous to the single-objective case, but has the disadvantage that analytical formulas for the Pareto front and Pareto set might not be available. The motivation behind this approach is that in practice, multiobjective problems are constructed in exactly this way—with each objective corresponding to a separate single-objective function. Concretely, we propose a generic way to combine the well-understood single-objective functions from the `bbob` test suite (Hansen et al., 2009). Using the well-established `bbob` test functions as building blocks allows us to build upon a careful statistical choice of the functions (without overrepresenting a certain type of problem) as well as comprehensive difficulties. In particular, our proposal fulfills all five recommendations for benchmark suites mentioned by Huband et al. (Huband et al. (2006), page 485). We showcase our idea by implementing two bi-objective test suites within the COCO platform (Hansen et al., 2016a) that supports automated benchmarking. The disadvantage of having no analytical expressions for the Pareto sets and Pareto fronts in our approach is addressed by visually displaying the approximations of Pareto sets and Pareto fronts coming from many numerical experiments with a large variety of algorithms. The corresponding hypervolume values are available online for performance assessment [2]. Moreover, the non-existence of analytical forms of Pareto set and Pareto front in our approach can be even seen as an advantage: the combination of existing single-objective test functions allows, in a controlled way, to mimic the typical constructions of real-world problems and to empirically investigate the resulting Pareto set and Pareto front shapes from such constructions.

The proposed multiobjective benchmark functions come in the form of pseudo-random *instances*, which allows to deal easily with the following two, otherwise non-trivial, tasks in performance assessment:

- the comparison of algorithms with different success probabilities (in the sense of reaching certain quality levels of the Pareto set approximations) and

- the comparison of deterministic and stochastic approaches.

The paper is organized as follows. We start by outlining the fundamental definitions in multiobjective optimization and benchmarking in Section 2 before reviewing existing multiobjective benchmark suites and their properties in Section 3. Section 4 then introduces the main concepts behind the well-known single-objective `bbob` test suite and discusses the ideas of function groups, objective normalization and problem instances. Next, Section 5 proposes the concrete `bbob-biobj` and `bbob-biobj-ext` test suites and showcases some of the their functions by visualizing the best found solutions in the objective and search space. Detailed descriptions and links to visualizations for all proposed functions are provided in an accompanying extended version of this article, which can be found at `http://bbobbiobj.gforge.inria.fr/bbob-biobj-functions.pdf`. The paper concludes with a proposal for creating test suites for an arbitrary number of objectives in Section 6 and concluding remarks in Section 7.

[2] The best known hypervolume values for all supported test instances are available via the COCO platform at `https://github.com/numbbo/coco/blob/master/code-experiments/src/suite_biobj_best_values_hyp.c`

2 Preliminaries

In the following, we consider bi-objective, unconstrained **minimization** problems of the form

$$\min_{x \in \mathbb{R}^n} F(x) = (f_\alpha(x), f_\beta(x)),$$

where n is the number of variables of the problem (also called the problem dimension), $f_\alpha : \mathbb{R}^n \to \mathbb{R}$ and $f_\beta : \mathbb{R}^n \to \mathbb{R}$ are the two objective functions, and the $\min$ operator is related to the standard *dominance relation*. A solution $x \in \mathbb{R}^n$ is thereby said to *dominate* another solution $y \in \mathbb{R}^n$ if $f_\alpha(x) \leq f_\alpha(y)$ and $f_\beta(x) \leq f_\beta(y)$ hold and at least one of the inequalities is strict. Note that we adopt the notation f_α for the first objective (resp. f_β for the second objective) instead of f_1 and f_2 to avoid confusion with notations adopted within the single-objective `bbob` test suite.

Solutions which are not dominated by any other solution in the search space are called *Pareto-optimal* or *efficient solutions*. All Pareto-optimal solutions constitute the *Pareto set* of which an approximation is sought. The Pareto set's image in the objective space $F(\mathbb{R}^n)$ is called the *Pareto front*.

Two specific points in the objective space are important to mention. The *ideal point* is defined as the vector in objective space that contains the optimal F-value for each objective *independently*. More precisely, if $f_\alpha^{\mathrm{opt}} := \inf_{x \in \mathbb{R}^n} f_\alpha(x)$ and $f_\beta^{\mathrm{opt}} := \inf_{x \in \mathbb{R}^n} f_\beta(x)$, the ideal point is given by

$$z_{\mathrm{ideal}} = (f_\alpha^{\mathrm{opt}}, f_\beta^{\mathrm{opt}}).$$

The *nadir point* (in objective space) consists in each objective of the worst value obtained by a Pareto-optimal solution. More precisely, if we denote the set of Pareto optimal points by $\mathcal{P}$, the nadir point satisfies

$$z_{\mathrm{nadir}} = \left(\sup_{x \in \mathcal{P}} f_\alpha(x), \sup_{x \in \mathcal{P}} f_\beta(x) \right).$$

In the specific case where each of two objective functions has a unique global minimum (that is, a single point in the search space which maps to the global minimum function value),

$$z_{\mathrm{nadir}} = \left(f_\alpha(x_\beta^{\mathrm{opt}}), f_\beta(x_\alpha^{\mathrm{opt}}) \right),$$

where $x_\alpha^{\mathrm{opt}} = \arg\min f_\alpha(x)$ and $x_\beta^{\mathrm{opt}} = \arg\min f_\beta(x)$.

Note that all given definitions generalize trivially to problems with more than two objectives. When solving an unconstrained multiobjective problem as the above, often the goal is to find, with as few evaluations of F as possible, a set of non-dominated solutions which is (i) as large as possible and (ii) has objective values as close to the Pareto front as possible. [3] Alternatively, the goal can also be to maximize a given quality indicator, for example the hypervolume (Zitzler et al., 2003) of the set of all non-dominated solutions found so far (Brockhoff et al., 2016).

When an optimization algorithm approaches the above minimization problem, it actually does not solve the generic function F, but a concrete *instance* of F with a

[3] The distance in objective space is defined here in such a way that the nadir and ideal points have in each coordinate the distance of one. Note also that finding a set of non-dominated solutions as large as possible might not always be the ultimate goal, in particular if the number of objective functions is large.

concrete problem dimension and potentially other concrete inherent parameters. Each generic multiobjective function F should therefore be seen as a parametrized function $F^\theta : \mathbb{R}^n \to \mathbb{R}^m$ with parameter value $\theta \in \Theta$, a concrete problem dimension n, and a concrete number of objectives m, here $m = 2$. The parameter value θ determines a so-called *function instance*. For example, θ might encode the location of the optimum of a single-objective (parametrized) function f^θ, which means that different instances have shifted optima:

$$f^\theta : \mathbb{R}^n \to \mathbb{R}$$
$$\text{with } f^{x^{\text{opt}}}(x) = ||x - x^{\text{opt}}||^2$$

where x and $\theta = x^{\text{opt}}$ live both in $\mathbb{R}^n (= \Theta)$. Despite simple shifts in the search space as in the above example, other transformations such as search space rotations and shifts in the objective values might be defined by instances as well as it is done, for example, in the COCO platform. In order to simplify the handling of instances, we have a mapping from a problem's parameter θ to an integer such that we can talk about the first, second, third, ... instance of a problem where the integer instance number is then mapped to a concrete θ parameter. In the proposed multiobjective test suites, the multiobjective function instances are furthermore determined by the instances of the underlying single-objective functions.

3 Review of Existing Multiobjective Test Suites

Many multiobjective test suites have been proposed throughout the years. Here, we in particular discuss those that are scalable in the problem dimension and that are unconstrained or box-constrained and defined in the continuous domain—the focus of our proposal for a new benchmark suite.

The (evolutionary) multiobjective optimization field first performed numerical comparisons of algorithms on single, independently proposed test problems such as the problems by Kursawe (1991) and Fonseca and Fleming (1995), see for example (Tan et al., 2002), or on actual real-world studies, see for example (Van Veldhuizen and Lamont, 1998) for an early overview. A first attempt to create a consistent multiobjective test function *suite* with several problems with desired properties was, to the best of our knowledge, the work of Van Veldhuizen and Lamont (1999b,a). Van Veldhuizen and Lamont clearly stated the need for scalable test suites and emphasized that problems of a test suite should contain practically relevant features.

In the years that followed, several other scalable test suites have been proposed, of which the most established ones are

- the ZDT suite of Zitzler et al. (2000), scalable in the number of variables but with only two objectives,
- its rotated version, the IHR problem suite of Igel et al. (2007),
- the DTLZ suite of Deb et al. (2005), with seven problems, all scalable in the number of variables and objectives,
- the WFG suite of Huband et al. (2006) with nine scalable problems of various difficulties,
- the LZ suite of Li and Zhang (2009) containing problems with more complicated Pareto sets,

- the CEC2007 suite, combining and extending 13 existing test functions from the literature (Huang et al., 2007),
- the CEC2009 suite with 13 problems overall (Zhang et al., 2009), and finally
- the CEC2017 suite with 17 collected problems, tailored towards many-objective optimization (Cheng et al., 2017).

Most of these test suites have some desirable properties like well-understood Pareto sets and Pareto fronts with shapes of various kinds (linear, convex, concave, discontinuous). But they also possess artificial characteristics that stem from the easier construction of such problems—overrepresenting properties such as no or only few dependencies among variables, Pareto sets located exactly at the boundary constraints, and the differentiation between position and distance variables. Although, for example, the importance of non-separable test functions in single-objective test suites is unquestioned and even Deb (Deb (2001), page 353f.) states its significance, most proposed multiobjective test problems are still separable or mostly separable in the sense that a function is separable if it can be optimized variable by variable. Even though all test suites in the above list are scalable in the problem dimension, we rarely see performance studies that investigate the scaling of the algorithms with the problem dimension.

The arguably most complete paper on the topic of multiobjective benchmark problems to date is still the work of (Huband et al., 2006) where the authors (i) identify important properties test functions should have, (ii) discuss in detail all other available test suites at that time with respect to these properties, and (iii) finally propose a new, well-motivated test suite that avoids many pitfalls of other test suites. In particular, Huband et al. (see Huband et al. (2006), page 485) recommend that multiobjective test suites should, in addition to recommendations for single-objective test suites:

1. contain a few unimodal test problems to test convergence velocity relative to different Pareto optimal geometries and bias conditions,
2. cover the three core types of Pareto optimal geometries: degenerate Pareto optimal fronts, disconnected Pareto optimal fronts, and disconnected Pareto optimal sets,
3. have a majority of its test problems multimodal with a few deceptive problems,
4. have the majority of problems nonseparable, and
5. contain problems that are both nonseparable and multimodal to be representative of real-world problems.

All five recommendations are fulfilled for the test suites proposed in this paper. Similar to the single-objective `bbob` test functions, the WFG suite of (Huband et al., 2006) employs problem transformations that change the properties like (non-)separability, bias, and the shape of the Pareto front of underlying *raw* objective functions.

One common property of the above mentioned test suites is that their Pareto sets can be described in analytical form. This certainly has an advantage for performance assessment but it also restricts the types of real-world problem characteristics that can be captured with such functions.

However, in practice, multiobjective optimization problems are typically constructed by combining objective functions that are defined (and understood) independently such as cost and performance of a new product. The objective functions might thereby come from different domains and share or do not share common properties such as uni-/multimodality, (non-)separability, asymmetry, etc.

The idea of defining multiobjective test problems by combining single-objective test functions is therefore straightforward and has been proposed before, for example by Igel et al. (2007) and Horn et al. (2015). To create a benchmark suite with challenging properties observed in practice, we follow here the same path and combine some of the existing, well-established, and well-understood test functions of the `bbob` test suite to create new multiobjective test suites.

4 The Single-objective `bbob` Functions

The main idea behind the multiobjective test suites proposed in this paper is to take well-understood single-objective test functions with problem properties observed in practice and to combine them to form multiobjective problems. We choose the functions from the well established `bbob` test suite since they all

- have associated scientific questions that can be answered by running numerical experiments on them,
- are categorized into function groups depending on their properties, and finally
- already come in the form of function instances.

This section first discusses properties of real-world problems and how the `bbob` test suite balances different problem difficulties. It then gives more details about the `bbob` functions, their function groups and instances.

4.1 Real-World Function Properties

We present here in short the general properties of objective functions that are related to difficulties observed in real-world problems. It depends on these properties whether an optimization problem is easy or hard to solve. They build the basis of the function groups described later.

A *separable* function does not have any dependencies among its variables and can therefore be optimized by applying n independent one-dimensional optimizations along each coordinate axis while keeping the other variables fixed. Difficult optimization problems are typically not separable and thus, *non-separable* optimization problems should be considered. The typical well-established technique to generate non-separable benchmark functions from separable ones is the application of a rotation matrix. That is, if $g(x)$ is a separable function with respect to x and $\mathbf{R} \in \mathbb{R}^{n \times n}$ is a rotation matrix, then $g(\mathbf{R}x)$ will generally be non-separable with respect to x.

A *unimodal* function has only one local minimum which is at the same time also its global one. A *multimodal* function has more local minima which is highly common in practical optimization problems. We consider a multimodal function to have *weak global structure* if the qualities (the f-values) of the local optima are only weakly related with their locations in search space, e.g. when neighboring optima do not generally have similar quality values.

Ill-conditioning is another typical challenge of real-parameter optimization and, besides multimodality, probably the most common one. The condition number measures,

loosely speaking, how strongly the steepness of the gradient depends on the position within a level set. The condition number measures in essence a variation of sensitivity, with a minimal value of 1. A small condition number means that the function is well-conditioned, while a large condition number indicates an ill-conditioned function. Conditioning can be rigorously formalized in the case of convex quadratic functions (with optimum in zero WLOG), $f(x) = \frac{1}{2}x^T Hx$ where H is a symmetric positive definite matrix, as the condition number of the Hessian matrix H. Since contour lines associated to a convex quadratic function are ellipsoids, the condition number corresponds to the squared ratio between the largest and the shortest axis length of the ellipsoid.

The `bbob` test suite contains ill-conditioned functions with a typical conditioning of 10^6. We believe this is a realistic requirement, while we have seen practical problems with conditioning as large as 10^{10} (Collange et al., 2010).

4.2 Balancing Problem Difficulties

It is worth noting that in several existing single-objective test suites, some of the easier properties are overrepresented. For example, in the CUTEr/CUTEst test suite (Gould et al., 2005), 202 (54%) out of the 375 functions, that are labeled as unconstrained or bound constrained, are of the "sum of squares" type, a further 58 (15%) are quadratic. Furthermore, out of the 191 problems with a fixed dimension, there are 49 (26%) that have only two variables while only 31 (16%) have a dimension larger than 10.

Such an overrepresentation is not a big problem per se, but when making statements on algorithm performance aggregated over all functions in a suite, one has to keep in mind that the performance of the better algorithms might simply come from the fact that they are tailored towards simpler problems.

With the `bbob` test suite, all problems are scalable in dimension and belong to a certain problem group, sharing similar difficulties. It is therefore possible to aggregate performance data only over a subset of the functions sharing the same properties. Having all problem groups of similar size also avoids problems of overfitting to certain difficulties if aggregated results are presented.

4.3 Function Groups

Related to the mentioned problem difficulties above, the `bbob` test suite comes with 24 functions, split into five function groups:

- Group 1 **Separable** contains only separable functions:
  - Sphere function (f_1 in the `bbob` suite)
  - Separable ellipsoid function (f_2 in the `bbob` suite)
  - Separable Rastrigin function (f_3 in the `bbob` suite)
  - Büche-Rastrigin function (f_4 in the `bbob` suite)
  - Linear slope function (f_5 in the `bbob` suite)
- Group 2 **Moderate** consists of functions with low or moderate conditioning, including multi-modal functions:
  - Attractive sector function (f_6 in the `bbob` suite)
  - Step ellipsoid function (f_7 in the `bbob` suite)
  - Original Rosenbrock function (f_8 in the `bbob` suite)
  - Rotated Rosenbrock function (f_9 in the `bbob` suite)

- Group 3 **Ill-conditioned** contains unimodal functions with high conditioning:
  - Ellipsoid function (f_{10} in the `bbob` suite)
  - Discus function (f_{11} in the `bbob` suite)
  - Bent cigar function (f_{12} in the `bbob` suite)
  - Sharp ridge function (f_{13} in the `bbob` suite)
  - Sum of different powers function (f_{14} in the `bbob` suite)
- Group 4 **Multi-modal** comprises multi-modal functions with adequate global structure:
  - Rastrigin function (f_{15} in the `bbob` suite)
  - Weierstrass function (f_{16} in the `bbob` suite)
  - Schaffer F7 function with condition number 10 (f_{17} in the `bbob` suite)
  - Schaffer F7 function with condition number 1000 (f_{18} in the `bbob` suite)
  - Composite Griewank-Rosenbrock function F8F2 (f_{19} in the `bbob` suite)
- Group 5 **Weakly-structured** consists of multi-modal functions with weak global structure:
  - Schwefel $x \sin x$ function (f_{20} in the `bbob` suite)
  - Gallagher 101 peaks function (f_{21} in the `bbob` suite)
  - Gallagher 21 peaks function (f_{22} in the `bbob` suite)
  - Katsuura function (f_{23} in the `bbob` suite)
  - Lunacek bi-Rastrigin function (f_{24} in the `bbob` suite)

See (Hansen et al., 2009) for the exact problem formulations. Problem difficulty is typically increasing from the first to the last group, but there are exceptions, for example, solving the Büche-Rastrigin function from the first group is quite difficult for most algorithms.

The main idea behind these hand-assigned function groups is that algorithm performance can be easily aggregated over all functions within a group in order to make meaningful statements on subsets of all 24 functions. If, for example, an application engineer knows that her/his real-world problem is multi-modal and also shows some global structure, a recommendation about which algorithm will perform well on that problem can be made mostly by looking at the multi-modal function group.

4.4 Function Instances

All `bbob` functions come naturally in the form of instances. That is to say, each function optimized by an algorithm takes the form:

$$f(x) = H_1 \circ \ldots \circ H_{k_1}(f_{\text{raw}}(T_1 \circ \ldots \circ T_{k_2}(x)))$$

where f_{raw} is a raw function—usually the simplest representative of the function class (like the sphere function with optimum in zero)—and where $T_i : \mathbb{R}^n \to \mathbb{R}^n$ are search space transformations and $H_i : \mathbb{R} \to \mathbb{R}$ are function value transformations that are applied to the raw function. For example search space transformations can be rotations or translations of the optimum and for example, a function-value transformation can

be translating the function by a scalar. Each of those transformations applied to the raw function are actually (pseudo)-random, e.g. when applying a translation in the search space, the vector by which the search point is shifted is randomly sampled. They can be seen as instances of a parametrized transformation.

In an abstract manner, the functions optimized are instances of a parametrized function F^θ (as introduced in Section 2); the parameter θ is instantiated (pseudo)-randomly from an integer number, the so-called instance number (and potentially function number). We refer to a function class as a set of functions $\{F^\theta : \theta \in \Theta\}$ and we often name the function class after its raw function.

Transformations that are shared by all `bbob` functions are shifts in the optimal function value and a pseudo-random location of the optimum. In addition, several of the non-separable functions are created by pseudo-random rotations of the search space and many of the simpler functions are made less regular by non-linear transformations in both search and objective space. See (Hansen et al., 2009) for more details.

Though the potential set of instances for a given `bbob` function is unbounded (and can be indexed by any positive integer), numerical benchmarking experiments are typically advised on 10–15 of those instances. Default instances in the COCO implementation might change from year to year to avoid overfitting. Note also that in some cases, single instances might be more difficult/easier to solve than others. However, in general, the difficulties among instances of the same `bbob` function are more similar than between different functions.

Performing numerical benchmarking experiments on a set of different instances of a parametrized function instead of experiments on a single fixed function has an immediate advantage: deterministic algorithms and stochastic algorithms can be compared easily in the same way stochastic algorithms are naturally compared. Running a deterministic algorithm on different instances of the same parametrized function introduces stochasticity of the runtime to reach certain target difficulties among runs in the same way than the combined stochasticity from the instance generation and the random events within a stochastic algorithm. Care, however, has to be taken that the variation of problem difficulty among instances is relatively low compared to the variation of difficulty between the actual benchmark functions [4].

4.5 Domain Bounds

All functions provided in the `bbob` suite are unbounded, i.e., defined on the entire real-valued space $\mathbb{R}^n$. The search domain of interest, however, is defined as $[-5, 5]^n$. With the exception of the linear slope (function f_5 in the `bbob` suite), the optimal solutions and hyperballs of radius 1 around them lie within the domain of interest for all instances in all dimensions.

4.6 Normalization and Target Difficulties

All `bbob` functions are normalized in the sense that the given target function values/difficulties around the optimal function value are comparable over functions and instances. Functions are provided with an f-offset such that the optimal function value is, loosely speaking, a realization of a Cauchy distribution with median zero and interquartile range 200. The optimal function value is furthermore rounded to two decimal places and set to ± 1000 if its absolute value exceeds 1000 (Hansen et al., 2009). The target difficulties are computed as a set of differences to the optimal function value.

[4] An assumption that does not always hold for all instances of highly multi-modal functions and that is not the case at all for instances of most combinatorial optimization problems.

The differences are equally spaced on the log scale and the same for all functions and instances. Algorithms however are not allowed to use or exploit any of this information (Hansen et al., 2016b).

5 The Proposed Bi-Objective Test Suites

The main contribution of this paper is the definition of multiobjective test suites by combining single-objective functions. For the bi-objective case and given the 24 single-objective bbob functions from Hansen et al. (2009), it is natural to combine all of them in pairs—resulting in $24^2 = 576$ bi-objective functions overall. We however assume that multiobjective optimization algorithms are not sensitive to permutations of the objective functions, so that there is no need to include the bi-objective function (f_β, f_α) if (f_α, f_β) is already present in the suite. This results in the total of $\binom{25}{2} = 300$ function combinations—the number of 2-combinations with repetitions, or 2-multicombinations of 24 objective functions [5].

While a benchmarking suite should contain a large number of different problems to avoid overfitting of algorithms to the problem suite, first tests in Brockhoff et al. (2015) showed that having 300 functions is impracticable in terms of the overall running time of a benchmarking experiment. Therefore, a subset of these 300 functions needed to be selected.

This section presents two such selections—the bbob-biobj test suite with 55 functions and its extension, the bbob-biobj-ext test suite with 92 functions. We also provide visualizations for some of the functions from the two suites here, showing different Pareto set and front shapes, while the plots for all 92 functions are collected in the accompanying paper at http://bbobbiobj.gforge.inria.fr/bbob-biobj-functions.pdf.

5.1 The bbob-biobj Test Suite

The bi-objective bbob-biobj test suite is created by exploiting the organization of the bbob functions into groups. More precisely, only two (representative) functions from each of the bbob function groups are chosen. This way, we do not introduce any bias towards a specific group. In addition, within each group, the functions are chosen to be the most representative without repeating similar functions. For example, only one Ellipsoid, one Rastrigin, and one Gallagher function are included in the bbob-biobj suite although they appear in multiple versions in the bbob suite.

Our choice of 10 bbob functions for creating the bbob-biobj test suite is the following:

- Separable functions:
  - Sphere function (f_1 in the bbob suite)
  - Separable ellipsoid function (f_2 in the bbob suite)
- Functions with low or moderate conditioning
  - Attractive sector function (f_6 in the bbob suite)
  - Original Rosenbrock function (f_8 in the bbob suite)
- Unimodal functions with high conditioning

[5] The general formula to compute the number $N_{k,s}$ of k-combinations with repetitions drawn from a ground set with s entries is $N_{k,s} = \binom{s+k-1}{k}$.

  - Sharp ridge function (f_{13} in the bbob suite)
  - Sum of different powers function (f_{14} in the bbob suite)

- Multi-modal functions with adequate global structure
  - Rastrigin function (f_{15} in the bbob suite)
  - Schaffer F7 function with condition number 10 (f_{17} in the bbob suite)

- Multi-modal functions with weak global structure
  - Schwefel $x \sin x$ function (f_{20} in the bbob suite)
  - Gallagher 101 peaks function (f_{21} in the bbob suite)

Using the previously described pairwise combinations, this results in having only $\binom{11}{2} = 55$ bi-objective functions in the final bbob-biobj suite (denoted as F_1 to F_{55} in the rest of the paper). They are all scalable in the search space dimension and come in the form of instances as it is the case with the original bbob suite.

In the following, we specify the common properties of the bbob-biobj functions and the main rationale behind them while concrete details on each of the 55 functions are given in the accompanying paper at http://bbobbiobj.gforge.inria.fr/bbob-biobj-functions.pdf. See Fig. 1 for an overview of how the single-objective functions (denoted with f_i) are combined to form the bi-objective functions of the bbob-biobj test suite.

5.1.1 Domain and Region of Interest

Since we use the single-objective bbob functions to construct the bbob-biobj suite, all functions are unbounded and the extreme solutions of the Pareto set are guaranteed to lie within $[-5, 5]^n$.

Note that the Pareto set can partially lie outside of this area but that the major part of the Pareto set is expected to lie within it. Moreover, it is highly unlikely that any non-dominated solutions would be found outside of the *region of interest* $[-100, 100]^n$. In other words, we believe that the region of interest contains the entire Pareto set, but due to the nature of the bbob-biobj function definitions, there is no guarantee that this is indeed always the case.

5.1.2 Function Groups

By combining the original bbob function groups, we obtain 15 function groups to structure the 55 bi-objective functions of the bbob-biobj test suite. Each function group contains three or four functions. We are listing below the function groups and in parenthesis the functions that belong to the respective groups (see also Fig. 1):

1. separable - separable (functions F_1, F_2, F_{11})
2. separable - moderate (F_3, F_4, F_{12}, F_{13})
3. separable - ill-conditioned (F_5, F_6, F_{14}, F_{15})
4. separable - multi-modal (F_7, F_8, F_{16}, F_{17})
5. separable - weakly-structured (F_9, F_{10}, F_{18}, F_{19})
6. moderate - moderate (F_{20}, F_{21}, F_{28})

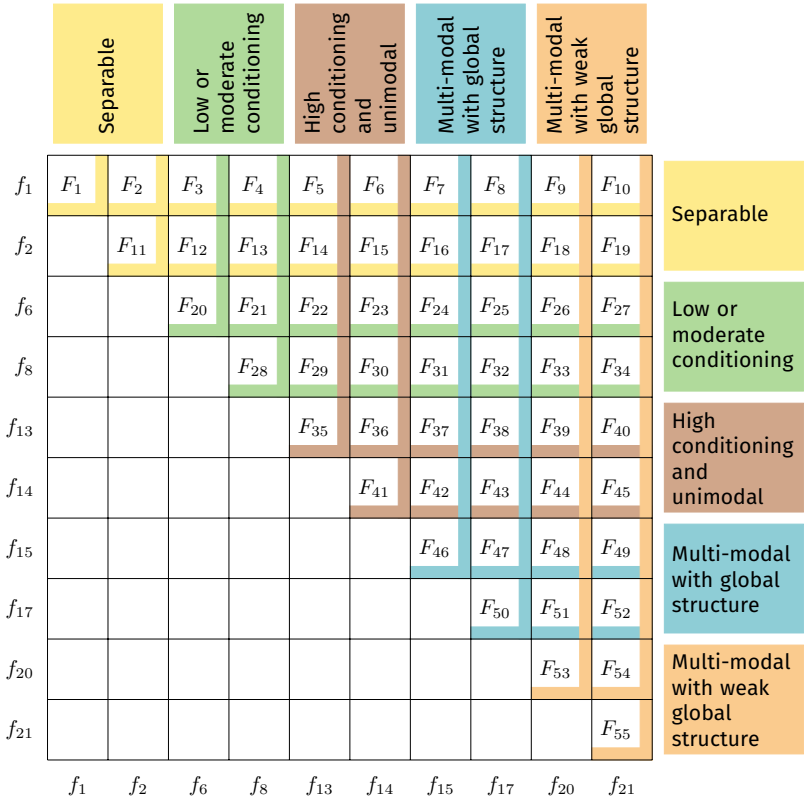

Figure 1: The functions of the `bbob-biobj` test suite (F_1 to F_{55}, in the table cells) together with the information about which single-objective `bbob` functions are used to define them (left and bottom annotations).

7. moderate - ill-conditioned (F_{22}, F_{23}, F_{29}, F_{30})
8. moderate - multi-modal (F_{24}, F_{25}, F_{31}, F_{32})
9. moderate - weakly-structured (F_{26}, F_{27}, F_{33}, F_{34})
10. ill-conditioned - ill-conditioned (F_{35}, F_{36}, F_{41})
11. ill-conditioned - multi-modal (F_{37}, F_{38}, F_{42}, F_{43})
12. ill-conditioned - weakly-structured (F_{39}, F_{40}, F_{44}, F_{45})
13. multi-modal - multi-modal (F_{46}, F_{47}, F_{50})
14. multi-modal - weakly structured (F_{48}, F_{49}, F_{51}, F_{52})
15. weakly structured - weakly structured (F_{53}, F_{54}, F_{55})

5.1.3 Normalization of Objectives

None of the 55 `bbob-biobj` functions is explicitly normalized and the optimization algorithms therefore have to cope with objective values in different ranges. Typically, different orders of magnitude between the objective values can be observed.

However, to facilitate comparison of algorithm performance over different functions, we suggest to normalize the objectives based on the ideal and nadir points before calculating the hypervolume indicator (Brockhoff et al., 2016). Both points can be computed, because the global optimum is known and is unique for the used 10 `bbob` base functions. In the black-box optimization benchmarking setup, the algorithm is allowed to use the values of the nadir point as an upper bound on the region of interest in objective space.

5.1.4 Instances

Our proposed test functions are parametrized and their instances are instantiations of the underlying parameters as is done for the `bbob` functions (see Hansen et al. (2016a)). The instances for the bi-objective functions are obtained using instances of each single-objective function composing the bi-objective one. In addition, we assert two conditions:

1. The Euclidean distance between the two single-objective optimal solutions (also called the extreme solutions) in the search space is at least 10^{-4}.

2. The Euclidean distance between the ideal and the nadir point in the non-normalized objective space is at least 10^{-1}.

We associate to each function instance an integer instance ID. The relation between the instance ID, K^F_{ID}, of a bi-objective function $F = (f_\alpha, f_\beta)$ and the instance IDs, $K^{f_\alpha}_{\mathrm{ID}}$ and $K^{f_\beta}_{\mathrm{ID}}$, of its underlying single-objective functions f_α and f_β is the following:

- $K^{f_\alpha}_{\mathrm{ID}} = 2K^F_{\mathrm{ID}} + 1$ and
- $K^{f_\beta}_{\mathrm{ID}} = K^{f_\alpha}_{\mathrm{ID}} + 1$

If we find that the two above conditions are not satisfied for all dimensions and functions in the `bbob-biobj` suite, we increase the instance ID of the second objective successively until both properties are fulfilled. For example, the `bbob-biobj` instance

ID 8 corresponds to the instance ID 17 for the first objective and instance ID 18 for the second objective. For the bbob-biobj instance ID 9, on the contrary, the first instance ID is 19 but for the second objective, instance ID 21 is chosen instead of instance ID 20 in order to conform with both conditions.

Exceptions to the above rule are, for historical reasons, the bbob-biobj instance IDs 1 and 2 in order to match the instance IDs 1 to 5 with the ones proposed in Brockhoff et al. (2015). The bbob-biobj instance ID 1 contains the single-objective instance IDs 2 and 4 and the bbob-biobj instance ID 2 contains the two instance IDs 3 and 5.

For each bi-objective function and given dimension, the bbob-biobj suite contains by default 15 instances. [6]

Problem instances in the multiobjective case can differ more wildly than those in the single-objective case. Even when for each single objective the different instances are similar, different combinations of them can result in different shapes of the Pareto front (for example continuous vs. discontinuous) or in different difficulties to solve such problems (the orientation of level sets, for example, might be in accordance between the objectives or perpendicular—resulting in significantly different multiobjective problems when two highly-conditioned functions are combined). [7] Consequently, we do not adopt the technique from the single-objective case to compare results from different instance sets. Yet it may well be possible to cherry-pick instances carefully to generate multiple sets with sufficiently uniform characteristics.

5.2 The bbob-biobj-ext Test Suite

Having all combinations of only a subset of the single-objective bbob functions in a test suite like the above bbob-biobj one has its advantages but also a few disadvantages. Using only a subset of the 24 bbob functions introduces a bias towards the chosen functions and reduces the amount of different difficulties a bi-objective algorithm is exposed to in the benchmarking exercise. Allowing all combinations of (a subset of the) bbob functions also increases the percentage of problems for which both objectives are from different bbob function groups. In practice, however, it can often be assumed that both objective functions come from a similar "function domain".

The rationale behind the extended test suite, denoted as bbob-biobj-ext, is therefore to reduce the mentioned effects. To this end, we add all within-group combinations of bbob functions which are not already in the bbob-biobj suite and which do not combine a function with itself. For technical reasons, we also remove the Weierstrass function (f_{16} in the bbob suite) because its optimum is not necessarily unique and computing the nadir point is therefore technically more challenging than for the other functions. This extension adds $3{\cdot}(4{+}3{+}2{+}1{-}1){+}2{\cdot}(3{+}2{+}1{-}1) = 3{\cdot}9{+}2{\cdot}5 = 37$ functions, resulting in 92 functions overall.

Fig. 2 details which single-objective bbob functions (left and bottom annotations) are contained in the 92 bbob-biobj-ext functions. Note that the numbers of the

[6] In principle, as for the instance generation for the bbob suite, the number of possible instances for the bbob-biobj suite is unlimited (Hansen et al., 2016a). However, running some tests with too few instances will render the potential statistics and their interpretation problematic while even the tiniest observed difference can be made statistically significant with a high enough number of instances. A good compromise to avoid either pitfall seems to lie between, say, 9 and 19 instances.

[7] While we cannot give a guarantee about the maximal difference in difficulty between instances, numerical experiments show that performance differences up to two orders of magnitude (in the number of function evaluations to reach a certain hypervolume indicator precision) can be observed in some cases. Differences of more than one order of magnitude happen in maximally 30% of the function/dimension pairs with typical algorithms on the proposed bbob-biobj test suite. Due to the higher amount of multimodal functions in the bbob-biobj-ext suite, differences among instances are more common.

first 55 bbob-biobj-ext functions are the same as in the bbob-biobj test suite for compatibility reasons.

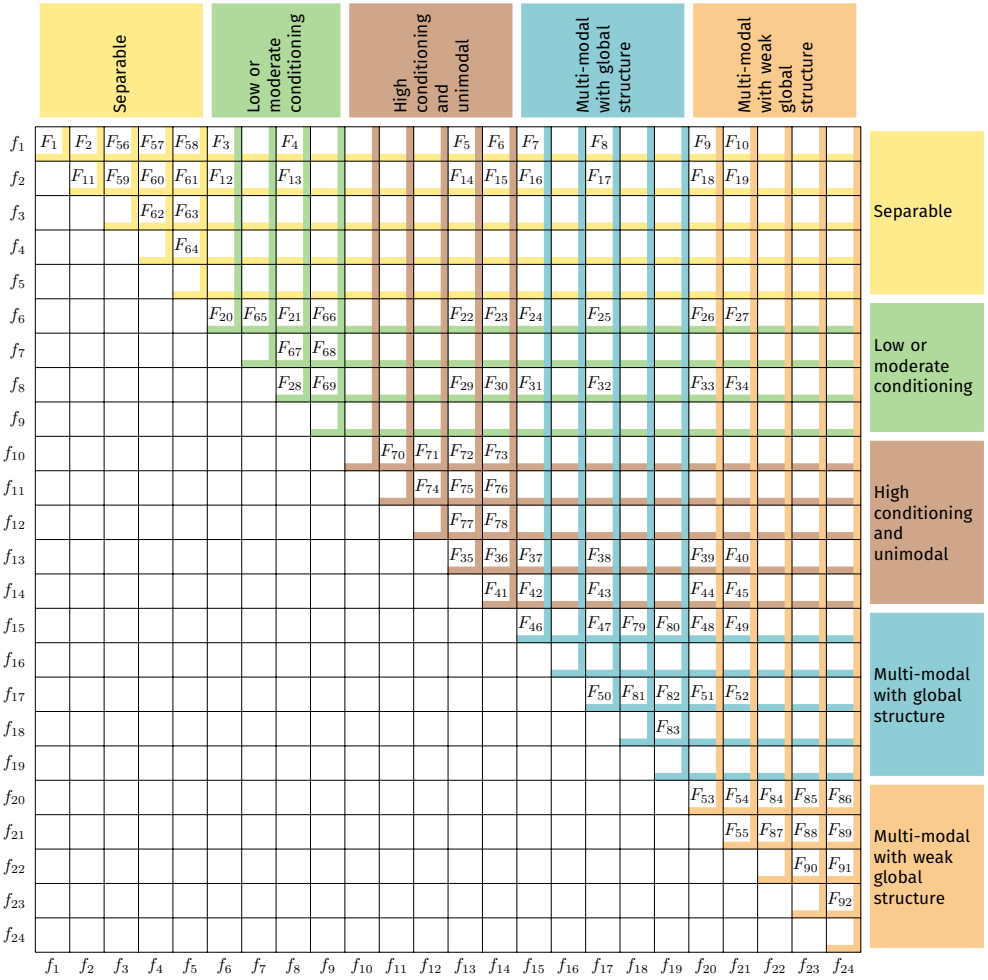

Figure 2: The functions of the bbob-biobj-ext test suite (F_1 to F_{92}, in the table cells) together with the information about which single-objective bbob functions are used to define them (left and bottom annotations).

5.2.1 Function Groups

Like for the bbob-biobj test suite, we obtain 15 function groups to structure the 92 bi-objective functions of the bbob-biobj-ext test suite. Depending on whether a function group combines functions from the same or from different bbob function groups, each function group contains 8, 12 or just four functions. We are listing below the function groups and in parenthesis the functions that belong to the respective group:

1. separable - separable (12 functions: F_1, F_2, F_{11}, F_{56}-F_{64})
2. separable - moderate (F_3, F_4, F_{12}, F_{13})

3. separable - ill-conditioned (F_5, F_6, F_{14}, F_{15})
4. separable - multi-modal (F_7, F_8, F_{16}, F_{17})
5. separable - weakly-structured (F_9, F_{10}, F_{18}, F_{19})
6. moderate - moderate (8 functions: F_{20}, F_{21}, F_{28}, F_{65}-F_{69})
7. moderate - ill-conditioned (F_{22}, F_{23}, F_{29}, F_{30})
8. moderate - multi-modal (F_{24}, F_{25}, F_{31}, F_{32})
9. moderate - weakly-structured (F_{26}, F_{27}, F_{33}, F_{34})
10. ill-conditioned - ill-conditioned (12 functions: F_{35}, F_{36}, F_{41}, F_{70}-F_{78})
11. ill-conditioned - multi-modal (F_{37}, F_{38}, F_{42}, F_{43})
12. ill-conditioned - weakly-structured (F_{39}, F_{40}, F_{44}, F_{45})
13. multi-modal - multi-modal (8 functions: F_{46}, F_{47}, F_{50}, F_{79}-F_{83})
14. multi-modal - weakly structured (F_{48}, F_{49}, F_{51}, F_{52})
15. weakly structured - weakly structured (12 functions: F_{53}-F_{55}, F_{84}-F_{92})

5.2.2 Normalization and Instances

Normalization of the objectives and instances for the `bbob-biobj-ext` test suite is handled in the same manner as for the `bbob-biobj` suite, i.e., the objective functions are not normalized and 15 instances are prescribed for a typical experiment.

5.3 Search Space and Objective Space Plots

In order to better understand the properties of the 55 `bbob-biobj` functions, we visualize the best known Pareto set and Pareto front approximations in the search and objective space, respectively, providing two plots for each (the approximations are depicted as black points). The first plot of the search space shows the projection onto a coordinate-axes-parallel cut defined by two variables, while the second plot contains the projection onto a random cutting plane which contains both single-objective optima. This second plot additionally shows the contour lines for both objective functions. Next, the first plot of the objective space is in original scaling (as seen by the algorithm), while the second is in log-scale, normalized so that the ideal point is at $(0, 0)$ and the nadir point is at $(1, 1)$.

In addition to the best known Pareto set/Pareto front approximations (in black), all plots show various cuts through the search space: (i) along a random direction through each single-objective optimum (in blue), (ii) along each coordinate axis through each single-objective optimum (blue dotted lines), (iii) along the line connecting both single-objective optima (in red), (iv) two fully random lines [8] (in yellow), and (v) a random line in the random projection plane going through both optima [9] (in green).

All lines are normalized (of length 10, where the support vector is in the middle). Ticks along the lines indicate the ends of line segments of the same length in search space. Thicker points on the lines depict solutions that are non-dominated with respect

[8] of random direction and with a support vector, drawn uniformly at random in $[-4, 4]^n$

[9] with a random direction within the plane and a support vector, drawn uniformly at random in $[-4, 4]$ in the coordinate system of the cutting plane

to all points on the same line. Furthermore, the search space plots highlight the projected region $[-5, 5]^n$ as a gray-shaded area while the gray-shaded area in the objective space plots denotes the region of interest between the ideal ($\times$) and nadir points ($+$). Note that, to keep the plots at a manageable size, the Pareto set and Pareto front approximations are carefully downsampled such that only one solution per grid point is shown—with the precision of 2 decimals for the search space plots and 3 decimals for the objective space plots to define the grid. The number of all available and actually displayed solutions is indicated in the legend of each plot.

The figure below shows exemplary plots for three functions of the `bbob-biobj` suite, the double sphere problem (F_1) with a continuous Pareto front and a straight line as the Pareto set, the sphere/Gallagher problem (F_{10}) with a continuous Pareto front but a gap in the Pareto set, and the double Rastrigin problem (F_{46}) for which both Pareto set and Pareto front are discontinuous. Due to downsampling, the number of displayed points ($\sim$ 10000 or less) is much smaller than the number of non-dominated solutions contained in the Pareto set approximation (2.9×10^6 for F_1, 1.5×10^6 for F_{10} and 3.1×10^5 for F_{46}). For links to the illustrations of *all* `bbob-biobj` and `bbob-biobj-ext` functions, we refer to the accompanying paper at `http://bbobbiobj.gforge.inria.fr/bbob-biobj-functions.pdf` and the accompanying web page `http://bbobbiobj.gforge.inria.fr/`. All plots shown and linked in this paper are provided only for the first instance of dimension 5, but further plots for more instances and dimensions are provided online at `http://bbobbiobj.gforge.inria.fr/`. This web page also provides the link to the python source code that was used to produce the plots.

6 Extension to Any Number of Objectives

The above proposed test suites are defined for two objective functions. There is however no general restriction of the proposed construction to only two objective functions. Yet, the number of resulting test problems will be practically too high if we extend the `bbob-biobj` and `bbob-biobj` suites naively.

The naive approach of combining all potential $s = 24$ `bbob` functions with each other (with repetitions but without caring about the order of the chosen functions), results in $\binom{s+m-1}{m}$ m-objective problems overall—which equals the number of m-combinations with repetitions, or m-multicombinations of s objective functions. Even restricting the number of used objective functions to $s = 10$, like in the `bbob-biobj` suite, results in $\binom{10+3-1}{3} = 220$ combinations for three objectives, $\binom{10+4-1}{4} = 715$ combinations for four objectives and $\binom{10+5-1}{5} = 2\,002$ combinations for five objectives. Multiplied by the six dimensions and 15 instances as recommended above, this would require 180 180 experiments to run the entire `bbob-biobj` suite in five objectives—an unsuitable number for practical experiments.

The goal is therefore to find an approach for combining single-objective functions to form m-objective problems that results in a suite of manageable size that contains different combinations of real-world function properties. Here, we suggest to follow the construction of the `bbob-biobj-ext` suite and define a number of function groups (dependent on the number of objectives m) while restricting the number of problems within one group. With this approach, the combinatorial explosion of the number of produced m-objective problems is less pronounced than with a naive approach, i.e., problem suites with up to eight objectives still have reasonable size.

Concretely, we propose the following multiobjective test suite *generator* to define multiobjective test suites with m objective functions and arbitrary dimensions and in-

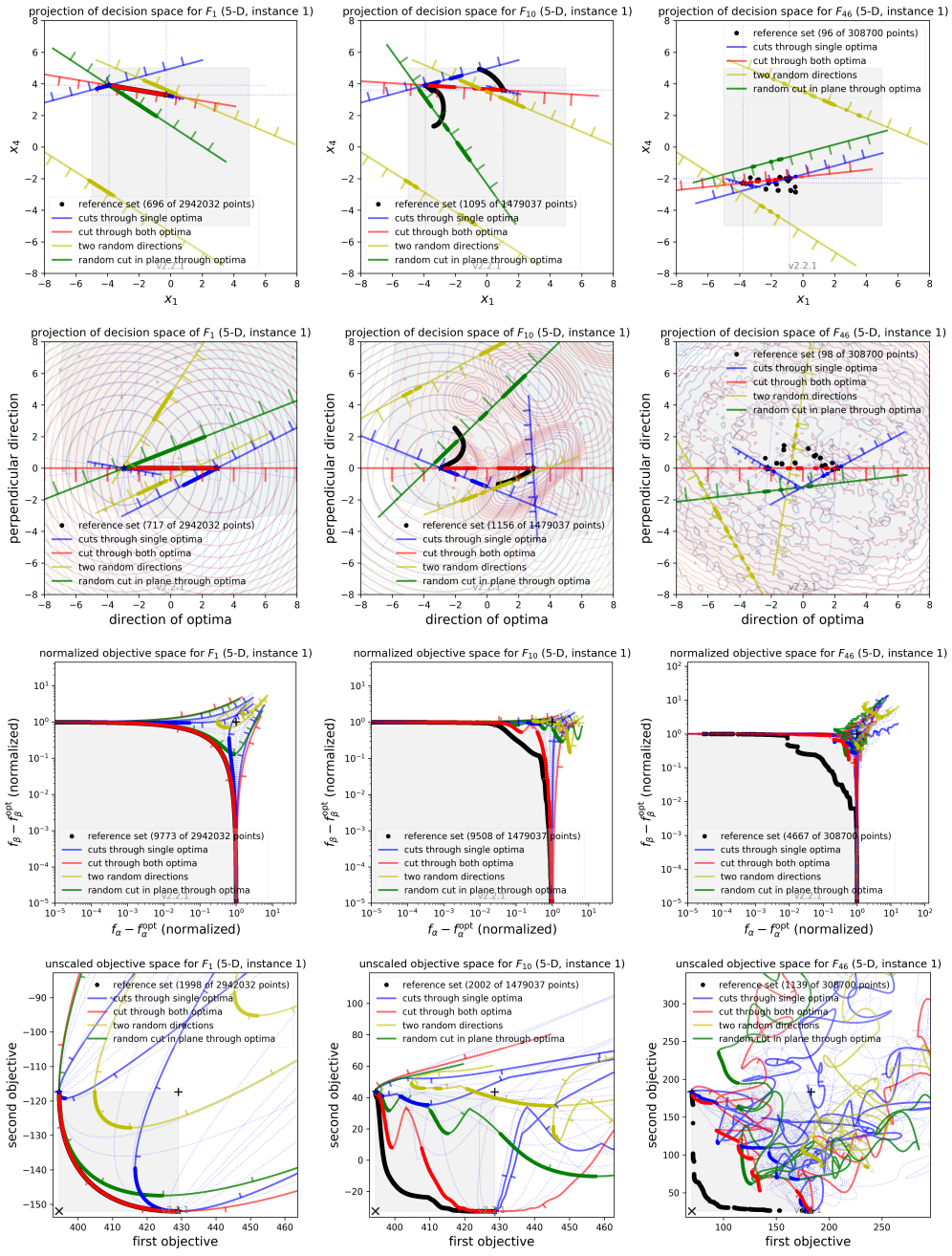

Figure 3: Illustration of the search space (first two rows) and the objective space (third row: normalized in log-scale; forth row: original scaling) for `bbob-biobj` functions F_1 (left column), F_{10} (middle column), and F_{46} (right column) in dimension 5 for the first instance.

stances. First, we define $\binom{5+m-1}{m}$ function groups by assigning to each of the m objective functions one of the five bbob function groups (with repetitions but without caring about the order). This will result in groups such as *separable - separable - separable* or *separable - ill-conditioned - multimodal* for three objectives. Then, we fill these function groups by sampling for each objective uniformly at random a bbob function from the corresponding single-objective function group (with the exception of f_{16}, as before). Following the structure of the bbob-biobj-ext suite, we recommend to produce more problems when all objective functions are from the same function group and significantly less for the other groups. Concretely, we suggest to sample 12 functions when the function group of all objectives is *separable*, *ill-conditioned* or *weakly-structured* and 8 functions when the function group of all objectives is *moderate* or *multi-modal*. In the cases where all objectives' function groups are different, we sample only four problems and in all other cases, we sample only twice. This way, we reproduce the structure of the bbob-biobj-ext suite when the number of objectives is two but reduce the number of problems in the suite in higher dimensions.

Since with six objectives or more, all objectives cannot come from different function groups, our construction results in $12+8+12+8+12+2\cdot(\binom{5+m-1}{m}-5)$ functions in total if $m > 5$. The proposed multiobjective suite will therefore have 462 (parametrized) functions for six objectives, 702 for seven objectives, 1032 for eight objectives, and so forth. These numbers are still very high, especially since multiple search space dimensions and instances need to be considered. For example, a 'standard' setting of the bbob-biobj suite comprises six dimensions and 15 instances per function. Running experiments with only four dimensions and five instances, however, would result in a (more) reasonable number of $462 \cdot 4 \cdot 5 = 9\,240$ experiments for a six-objective test suite compared to the naive approach with $\binom{10+6-1}{6} \cdot 4 \cdot 5 = 100\,100$ experiments. Note that, in comparison, an entire experiment on the 92 bbob-biobj-ext functions with six dimensions and 15 instances also corresponds to already $92 \cdot 6 \cdot 15 = 8\,280$ single experiments.

Note that the random choice of objective functions should rather be pseudo-random in an actual implementation of the proposed multiobjective suite. The random seed to sample the objective functions can be chosen as the objective function index plus a given constant, e.g. $100\,000 + i$ to sample the objective function $\bar{f}_i$ of an m-objective function $F = (\bar{f}_1, \ldots, \bar{f}_i, \ldots, \bar{f}_m)$. Exceptions to this rule are expected, for example, in order to always have the well-understood multi-sphere function [10] in the test suite or to have the bbob-biobj-ext suite become a special case of the general multiobjective suite if the number of objectives is two.

7 Conclusions

Designing test suites is a crucial part of benchmarking optimization algorithms. Arguably, the most problematic aspect of using *artificial* test functions to assess performance is the *representativeness* of these regarding difficulties observed in real-world problems. In this paper, we suggest to address the problem of representativeness in the multiobjective case by combining established single-objective test functions with known difficulties observed in practice. Following the concepts of the single-objective bbob test suite, we propose two concrete bi-objective test suites and a test suite *generator* for arbitrary numbers of objectives based on the same idea of combining existing single-objective functions.

[10] In which each objective is an instance of the sphere function.

Table 1: Concrete numbers for the size of the test function suites when combining the `bbob` functions (without the Weierstrass function) to m-objective problems. The *all combinations* column gives the numbers $\binom{s+m-1}{m}$ for the naive implementation with all possible function combinations (of either $s = 10$ or $s = 23$ `bbob` functions) and the *proposed suite construction* column gives the numbers for the approach proposed here which decides first on the objectives' function groups and then samples functions from the groups with the number of objectives in the first column. If we assume that the test suites contain scalable problems in n_d different dimensions with n_i instances per function/dimension pair, the given numbers must be multiplied by $n_d \cdot n_i$.

#obj	all combinations (with repetitions)		proposed suite construction
	based on 10 functions	based on 23 functions	based on 23 functions
2	55	276	92
3	220	2,300	132
4	715	14,950	192
5	2,002	80,730	296
6	5,005	376,740	462
7	11,440	1,560,780	702
8	24,310	5,852,925	1,032
9	48,620	20,160,075	1,472
10	92,378	64,512,240	2,044

Our approach contrasts most of the existing test suites for multiobjective optimization. These are based on the desirable property of having well-understood Pareto sets and Pareto fronts with analytical forms but have, on the other hand, artificial characteristics that are arguably under-represented in real-world problems. Examples of such properties are separability, optima located exactly at the boundary constraints, and the existence of variables that solely control the distance between a solution and the Pareto front.

The disadvantage of unknown analytical forms of the Pareto sets and Pareto fronts in our proposal is addressed by collecting the non-dominated solutions from extensive experiments with dozens of different optimization algorithms and providing and visualizing the Pareto set and Pareto front approximations for each problem. These visualizations lead to new insights into how such non-analytical Pareto sets and Pareto fronts may look in practice.

Acknowledgments

This work was supported by the grant ANR-12-MONU-0009 (NumBBO) of the French National Research Agency. We also thank Ilya Loshchilov and Oswin Krause for their initial suggestions on how to extend the `bbob-biobj` test suite.

Tea Tušar acknowledges the financial support from the Slovenian Research Agency (project No. Z2-8177). This work is part of a project that has received funding from the *European Union's Horizon 2020 research and innovation program* under grant agreement No.692286.

References

Brockhoff, D., Tran, T.-D., and Hansen, N. (2015). Benchmarking Numerical Multiobjective Optimizers Revisited. In *Genetic and Evolutionary Computation Conference (GECCO 2015)*, pages 639–646. ACM.

Brockhoff, D., Tušar, T., Tušar, D., Wagner, T., Hansen, N., and Auger, A. (2016). Biobjective Performance Assessment with the COCO Platform. *CoRR*, abs/1605.01746.

Cheng, R., Li, M., Tian, Y., Zhang, X., Yang, S., Jin, Y., and Yao, X. (2017). Benchmark functions for the cec'2017 competition on many-objective optimization. Technical report, University of Birmingham, UK.

Collange, G., Delattre, N., Hansen, N., Quinquis, I., and Schoenauer, M. (2010). Multidisciplinary Optimisation in the Design of Future Space Launchers. In *Multidisciplinary Design Optimization in Computational Mechanics*, pages 487–496. Wiley.

Deb, K. (2001). *Multi-Objective Optimization Using Evolutionary Algorithms*. Wiley, Chichester, UK.

Deb, K., Thiele, L., Laumanns, M., and Zitzler, E. (2005). Scalable Test Problems for Evolutionary Multi-Objective Optimization. In Abraham, A., Jain, R., and Goldberg, R., editors, *Evolutionary Multiobjective Optimization: Theoretical Advances and Applications*, chapter 6, pages 105–145. Springer.

Fonseca, C. M. and Fleming, P. J. (1995). An Overview of Evolutionary Algorithms in Multiobjective Optimization. *Evolutionary Computation*, 3(1):1–16.

Gould, N. I. M., Orban, D., and Toint, P. L. (2005). CUTEr and SifDec: A Constrained and Unconstrained Testing Environment, revisited. *ACM Transactions on Mathematical Software*, 29(4):373–394.

Hansen, N., Auger, A., Finck, S., and Ros, R. (2009). Real-Parameter Black-Box Optimization Benchmarking 2009: Experimental Setup. INRIA Research Report RR-6829, INRIA Saclay—Ile-de-France. updated February 2010.

Hansen, N., Auger, A., Mersmann, O., Tušar, T., and Brockhoff, D. (2016a). COCO: A Platform for Comparing Continuous Optimizers in a Black-Box Setting. *CoRR*, abs/1603.08785.

Hansen, N., Tušar, T., Mersmann, O., Auger, A., and Brockhoff, D. (2016b). COCO: The Experimental Procedure. *CoRR*, abs/1603.08776.

Horn, D., Wagner, T., Biermann, D., Weihs, C., and Bischl, B. (2015). Model-based multiobjective optimization: taxonomy, multi-point proposal, toolbox and benchmark. In *Evolutionary Multi-Criterion Optimization (EMO 2015)*, pages 64–78. Springer.

Huang, V. L., Qin, A. K., Deb, K., Zitzler, E., Suganthan, P. N., Liang, J. J., Preuss, M., and Huband, S. (2007). Problem Definitions for Performance Assessment of Multiobjective Optimization Algorithms. Technical report, Nanyang Technological University. Special Session on Constrained Real-Parameter Optimization.

Huband, S., Hingston, P., Barone, L., and While, L. (2006). A Review of Multiobjective Test Problems and a Scalable Test Problem Toolkit. *IEEE Transactions on Evolutionary Computation*, 10(5):477–506.

Igel, C., Hansen, N., and Roth, S. (2007). Covariance Matrix Adaptation for Multi-objective Optimization. *Evolutionary Computation*, 15(1):1–28.

Kursawe, F. (1991). A Variant of Evolution Strategies for Vector Optimization. In Schwefel, H.-P. and Männer, R., editors, *Conference on Parallel Problem Solving from Nature (PPSN I)*, pages 193–197. Springer.

Li, H. and Zhang, Q. (2009). Multiobjective Optimization Problems With Complicated Pareto Sets, MOEA/D and NSGA-II. *IEEE Transactions on Evolutionary Computation*, 13(2):284–302.

Tan, K. C., Lee, T. H., and Khor, E. F. (2002). Evolutionary algorithms for multi-objective optimization: Performance assessments and comparisons. *Artificial intelligence Review*, 17(4):251–290.

Van Veldhuizen, D. A. and Lamont, G. B. (1998). Multiobjective evolutionary algorithm research: A history and analysis. Technical Report TR-98-03, Department of Electrical and Computer Engineering, Graduate School of Engineering, Air Force Institute of Technology.

Van Veldhuizen, D. A. and Lamont, G. B. (1999a). Moea test suite generation, design & use. In *Proceedings of the 1999 Genetic and Evolutionary Computation Conference. Workshop Program*, pages 113–114.

Van Veldhuizen, D. A. and Lamont, G. B. (1999b). Multiobjective evolutionary algorithm test suites. In *Symposium on Applied Computing*, pages 351–357. ACM.

Zhang, Q., Zhou, A., Zhao, S., Suganthan, P. N., Liu, W., and Tiwari, S. (2009). Multiobjective Optimization Test Instances for the CEC 2009 Special Session and Competition. CES 487, The School of Computer Science and Electronic Engieering, University of Essex.

Zitzler, E., Deb, K., and Thiele, L. (2000). Comparison of Multiobjective Evolutionary Algorithms: Empirical Results. *Evolutionary Computation*, 8(2):173–195.

Zitzler, E., Thiele, L., Laumanns, M., Fonseca, C. M., and Grunert da Fonseca, V. (2003). Performance Assessment of Multiobjective Optimizers: An Analysis and Review. *IEEE Transactions on Evolutionary Computation*, 7(2):117–132.

8 Appendix

8.1 Definitions and Plots of the Proposed Functions

8.1.1 F_1: Sphere/Sphere

Combination of two sphere functions (f_1 in the `bbob` suite).
Both objectives are unimodal, highly symmetric, rotational and scale invariant. The Pareto set is known to be a straight line and the Pareto front is convex. Furthermore, the normalized hypervolume value of the entire Pareto front with respect to the nadir point as reference point can be computed analytically as the integral $1-\int_0^1 (1-\sqrt{x})^2 dx = -\frac{1}{2} + \frac{4}{3} = 0.833333\ldots$.

Considered as the simplest bi-objective problem in continuous domain. Contained in the *separable - separable* function group.

Links to illustrations of function F_1 in dimension 5 for the first instance:

- Search space plot along two coordinate axes
- Projection of the search space into a hyperplane through both optima
- Normalized objective space plot (in log-scale)
- Unscaled objective space plot

8.1.2 F_2: Sphere/Ellipsoid separable

Combination of the sphere function (f_1 in the `bbob` suite) and the separable ellipsoid function (f_2 in the `bbob` suite).

Both objectives are unimodal and separable. While the first objective is truly convex-quadratic with a condition number of 1, the second objective is only globally quadratic with smooth local irregularities and highly ill-conditioned with a condition number of about 10^6.

Contained in the *separable - separable* function group.

Links to illustrations of function F_2 in dimension 5 for the first instance:

- Search space plot along two coordinate axes
- Projection of the search space into a hyperplane through both optima
- Normalized objective space plot (in log-scale)
- Unscaled objective space plot

8.1.3 F_3: Sphere/Attractive sector

Combination of the sphere function (f_1 in the `bbob` suite) and the attractive sector function (f_6 in the `bbob` suite).

Both objective functions are unimodal, but only the first objective is separable and truly convex quadratic. The attractive sector function is highly asymmetric, where only one *hypercone* (with angular base area) with a volume of roughly $(1/2)^n$ yields low function values. The optimum of it is located at the tip of this cone.

Contained in the *separable - moderate* function group.

Links to illustrations of function F_3 in dimension 5 for the first instance:

- Search space plot along two coordinate axes
- Projection of the search space into a hyperplane through both optima
- Normalized objective space plot (in log-scale)
- Unscaled objective space plot

8.1.4 F_4: Sphere/Rosenbrock original

Combination of the sphere function (f_1 in the `bbob` suite) and the original, i.e., unrotated Rosenbrock function (f_8 in the `bbob` suite).

The first objective is separable and truly convex, the second objective is partially separable (tri-band structure). The first objective is unimodal while the second objective has a local optimum with an attraction volume of about 25%.

Contained in the *separable - moderate* function group.

Links to illustrations of function F_4 in dimension 5 for the first instance:

- Search space plot along two coordinate axes
- Projection of the search space into a hyperplane through both optima
- Normalized objective space plot (in log-scale)
- Unscaled objective space plot

8.1.5 F_5: Sphere/Sharp ridge

Combination of the sphere function (f_1 in the `bbob` suite) and the sharp ridge function (f_{13} in the `bbob` suite).

Both objective functions are unimodal. In addition to the simple, separable, and differentiable first objective, a sharp, i.e., non-differentiable ridge has to be followed for optimizing the (non-separable) second objective. The gradient towards the ridge remains constant, when the ridge is approached from a given point. Approaching the ridge is initially effective, but becomes ineffective close to the ridge when the ridge needs to be followed in direction to its optimum. The necessary change in *search behavior* close to the ridge is difficult to diagnose, because the gradient towards the ridge does not flatten out.

Contained in the *separable - ill-conditioned* function group.

Links to illustrations of function F_5 in dimension 5 for the first instance:

- Search space plot along two coordinate axes
- Projection of the search space into a hyperplane through both optima
- Normalized objective space plot (in log-scale)
- Unscaled objective space plot

8.1.6 F_6: Sphere/Sum of Different Powers

Combination of the sphere function (f_1 in the `bbob` suite) and the sum of different powers function (f_{14} in the `bbob` suite).

Both objective functions are unimodal. The first objective is separable, the second non-separable. When approaching the second objective's optimum, the difference in sensitivity between different directions in search space increases unboundedly.

Contained in the *separable - ill-conditioned* function group.

Links to illustrations of function F_6 in dimension 5 for the first instance:

- Search space plot along two coordinate axes
- Projection of the search space into a hyperplane through both optima
- Normalized objective space plot (in log-scale)
- Unscaled objective space plot

8.1.7 F_7: Sphere/Rastrigin

Combination of the sphere function (f_1 in the `bbob` suite) and the Rastrigin function (f_{15} in the `bbob` suite).

In addition to the simple sphere function, the prototypical highly multimodal Rastrigin function needs to be solved which has originally a very regular and symmetric structure for the placement of the optima. Here, however, transformations are performed to alleviate the original symmetry and regularity in the second objective.

The properties of the second objective contain non-separability, multimodality (roughly 10^n local optima), a conditioning of about 10, and a large global amplitude compared to the local amplitudes.

Contained in the *separable - multi-modal* function group.

Links to illustrations of function F_7 in dimension 5 for the first instance:

- Search space plot along two coordinate axes
- Projection of the search space into a hyperplane through both optima
- Normalized objective space plot (in log-scale)
- Unscaled objective space plot

8.1.8 F_8: Sphere/Schaffer F7, condition 10

Combination of the sphere function (f_1 in the `bbob` suite) and the Schaffer F7 function with condition number 10 (f_{17} in the `bbob` suite).

In addition to the simple sphere function, an asymmetric, non-separable, and highly multimodal function needs to be solved to approach the Pareto front/Pareto set where the frequency and amplitude of the modulation in the second objective vary. The conditioning of the second objective and thus the entire bi-objective function is low.

Contained in the *separable - multi-modal* function group.

Links to illustrations of function F_8 in dimension 5 for the first instance:

- Search space plot along two coordinate axes
- Projection of the search space into a hyperplane through both optima
- Normalized objective space plot (in log-scale)
- Unscaled objective space plot

8.1.9 F_9: Sphere/Schwefel x*sin(x)

Combination of the sphere function (f_1 in the `bbob` suite) and the Schwefel function (f_{20} in the `bbob` suite).

While the first objective function is separable and unimodal, the second objective function is partially separable and highly multimodal—having the most prominent 2^n minima located comparatively close to the corners of the unpenalized search area.

Contained in the *separable - weakly-structured* function group.

Links to illustrations of function F_9 in dimension 5 for the first instance:

- Search space plot along two coordinate axes
- Projection of the search space into a hyperplane through both optima
- Normalized objective space plot (in log-scale)
- Unscaled objective space plot

8.1.10 F_{10}: Sphere/Gallagher 101 peaks

Combination of the sphere function (f_1 in the `bbob` suite) and the Gallagher function with 101 peaks (f_{21} in the `bbob` suite).

While the first objective function is separable and unimodal, the second objective function is non-separable and consists of 101 optima with position and height being unrelated and randomly chosen (different for each instantiation of the function). The conditioning around the global optimum of the second objective function is about 30.

Contained in the *separable - weakly-structured* function group.

Links to illustrations of function F_{10} in dimension 5 for the first instance:

- Search space plot along two coordinate axes
- Projection of the search space into a hyperplane through both optima
- Normalized objective space plot (in log-scale)
- Unscaled objective space plot

8.1.11 F_{11}: Ellipsoid separable/Ellipsoid separable

Combination of two separable ellipsoid functions (f_2 in the `bbob` suite).

Both objectives are unimodal, separable, only globally quadratic with smooth local irregularities, and highly ill-conditioned with a condition number of about 10^6.

Contained in the *separable - separable* function group.

Links to illustrations of function F_{11} in dimension 5 for the first instance:

- Search space plot along two coordinate axes
- Projection of the search space into a hyperplane through both optima
- Normalized objective space plot (in log-scale)
- Unscaled objective space plot

8.1.12 F_{12}: Ellipsoid separable/Attractive sector

Combination of the separable ellipsoid function (f_2 in the `bbob` suite) and the attractive sector function (f_6 in the `bbob` suite).

Both objective functions are unimodal but only the first one is separable. The first objective function, in addition, is globally quadratic with smooth local irregularities, and highly ill-conditioned with a condition number of about 10^6. The second objective function is highly asymmetric, where only one *hypercone* (with angular base area) with a volume of roughly $(1/2)^n$ yields low function values. The optimum of it is located at the tip of this cone.

Contained in the *separable - moderate* function group.

Links to illustrations of function F_{12} in dimension 5 for the first instance:

- Search space plot along two coordinate axes
- Projection of the search space into a hyperplane through both optima
- Normalized objective space plot (in log-scale)
- Unscaled objective space plot

8.1.13 F_{13}: Ellipsoid separable/Rosenbrock original

Combination of the separable ellipsoid function (f_2 in the `bbob` suite) and the original, i.e., unrotated Rosenbrock function (f_8 in the `bbob` suite).

Only the first objective is separable and unimodal. The second objective is partially separable (tri-band structure) and has a local optimum with an attraction volume of about 25%. In addition, the first objective function shows smooth local irregularities from a globally convex quadratic function and is highly ill-conditioned with a condition number of about 10^6.

Contained in the *separable - moderate* function group.

Links to illustrations of function F_{13} in dimension 5 for the first instance:

- Search space plot along two coordinate axes
- Projection of the search space into a hyperplane through both optima
- Normalized objective space plot (in log-scale)
- Unscaled objective space plot

8.1.14 F_{14}: Ellipsoid separable/Sharp ridge

Combination of the separable ellipsoid function (f_2 in the `bbob` suite) and the sharp ridge function (f_{13} in the `bbob` suite).

Both objective functions are unimodal but only the first one is separable.

The first objective is globally quadratic but with smooth local irregularities and highly ill-conditioned with a condition number of about 10^6. For optimizing the second objective, a sharp, i.e., non-differentiable ridge has to be followed.

Contained in the *separable - ill-conditioned* function group.

Links to illustrations of function F_{14} in dimension 5 for the first instance:

- Search space plot along two coordinate axes
- Projection of the search space into a hyperplane through both optima
- Normalized objective space plot (in log-scale)
- Unscaled objective space plot

8.1.15 F_{15}: Ellipsoid separable/Sum of Different Powers

Combination of the separable ellipsoid function (f_2 in the `bbob` suite) and the sum of different powers function (f_{14} in the `bbob` suite).

Both objective functions are unimodal but only the first one is separable.

The first objective is globally quadratic but with smooth local irregularities and highly ill-conditioned with a condition number of about 10^6. When approaching the second objective's optimum, the sensitivities of the variables in the rotated search space become more and more different.

Contained in the *separable - ill-conditioned* function group.

Links to illustrations of function F_{15} in dimension 5 for the first instance:

- Search space plot along two coordinate axes
- Projection of the search space into a hyperplane through both optima
- Normalized objective space plot (in log-scale)
- Unscaled objective space plot

8.1.16 F_{16}: Ellipsoid separable/Rastrigin

Combination of the separable ellipsoid function (f_2 in the `bbob` suite) and the Rastrigin function (f_{15} in the `bbob` suite).

The objective functions show rather opposite properties. The first one is separable, the second not. The first one is unimodal, the second highly multimodal (roughly 10^n local optima). The first one is highly ill-conditioning (condition number of 10^6), the second one has a conditioning of about 10. Local non-linear transformations are performed in both objective functions to alleviate the original symmetry and regularity of the two baseline functions.

Contained in the *separable - multi-modal* function group.

Links to illustrations of function F_{16} in dimension 5 for the first instance:

- Search space plot along two coordinate axes
- Projection of the search space into a hyperplane through both optima
- Normalized objective space plot (in log-scale)
- Unscaled objective space plot

8.1.17 F_{17}: Ellipsoid separable/Schaffer F7, condition 10

Combination of the separable ellipsoid function (f_2 in the `bbob` suite) and the Schaffer F7 function with condition number 10 (f_{17} in the `bbob` suite).

Also here, both single objectives possess opposing properties. The first objective is unimodal, besides small local non-linearities symmetric, separable and highly ill-conditioned while the second objective is highly multi-modal, asymmetric, and non-separable, with only a low conditioning.

Contained in the *separable - multi-modal* function group.

Links to illustrations of function F_{17} in dimension 5 for the first instance:

- Search space plot along two coordinate axes
- Projection of the search space into a hyperplane through both optima
- Normalized objective space plot (in log-scale)
- Unscaled objective space plot

8.1.18 F_{18}: Ellipsoid separable/Schwefel x*sin(x)

Combination of the separable ellipsoid function (f_2 in the `bbob` suite) and the Schwefel function (f_{20} in the `bbob` suite).

The first objective is unimodal, separable and highly ill-conditioned. The second objective is partially separable and highly multimodal—having the most prominent 2^n minima located comparatively close to the corners of the unpenalized search area.

Contained in the *separable - weakly-structured* function group.

Links to illustrations of function F_{18} in dimension 5 for the first instance:

- Search space plot along two coordinate axes
- Projection of the search space into a hyperplane through both optima
- Normalized objective space plot (in log-scale)
- Unscaled objective space plot

8.1.19 F_{19}: Ellipsoid separable/Gallagher 101 peaks

Combination of the separable ellipsoid function (f_2 in the `bbob` suite) and the Gallagher function with 101 peaks (f_{21} in the `bbob` suite).

While the first objective function is separable, unimodal, and highly ill-conditioned (condition number of about 10^6), the second objective function is non-separable and consists of 101 optima with position and height being unrelated and randomly chosen (different for each instantiation of the function). The conditioning around the global optimum of the second objective function is about 30.

Contained in the *separable - weakly-structured* function group.

Links to illustrations of function F_{19} in dimension 5 for the first instance:

- Search space plot along two coordinate axes
- Projection of the search space into a hyperplane through both optima
- Normalized objective space plot (in log-scale)
- Unscaled objective space plot

8.1.20 F_{20}: Attractive sector/Attractive sector

Combination of two attractive sector functions (f_6 in the `bbob` suite). Both functions are unimodal and highly asymmetric, where only one *hypercone* (with angular base area) per objective with a volume of roughly $(1/2)^n$ yields low function values. The objective functions' optima are located at the tips of those two cones.

Contained in the *moderate - moderate* function group.

Links to illustrations of function F_{20} in dimension 5 for the first instance:

- Search space plot along two coordinate axes
- Projection of the search space into a hyperplane through both optima
- Normalized objective space plot (in log-scale)
- Unscaled objective space plot

8.1.21 F_{21}: Attractive sector/Rosenbrock original

Combination of the attractive sector function (f_6 in the `bbob` suite) and the Rosenbrock function (f_8 in the `bbob` suite).

The first function is unimodal but highly asymmetric, where only one *hypercone* (with angular base area) with a volume of roughly $(1/2)^n$ yields low function values (with the optimum at the tip of the cone). The second objective is partially separable (tri-band structure) and has a local optimum with an attraction volume of about 25%.

Contained in the *moderate - moderate* function group.

Links to illustrations of function F_{21} in dimension 5 for the first instance:

- Search space plot along two coordinate axes
- Projection of the search space into a hyperplane through both optima
- Normalized objective space plot (in log-scale)
- Unscaled objective space plot

8.1.22 F_{22}: Attractive sector/Sharp ridge

Combination of the attractive sector function (f_6 in the `bbob` suite) and the sharp ridge function (f_{13} in the `bbob` suite).

Both objective functions are unimodal and non-separable. The first objective is highly asymmetric in the sense that only one *hypercone* (with angular base area) with a volume of roughly $(1/2)^n$ yields low function values (with the optimum at the tip of the cone). For optimizing the second objective, a sharp, i.e., non-differentiable ridge has to be followed.

Contained in the *moderate - ill-conditioned* function group.

Links to illustrations of function F_{22} in dimension 5 for the first instance:

- Search space plot along two coordinate axes
- Projection of the search space into a hyperplane through both optima
- Normalized objective space plot (in log-scale)
- Unscaled objective space plot

8.1.23 F_{23}: Attractive sector/Sum of Different Powers

Combination of the attractive sector function (f_6 in the `bbob` suite) and the sum of different powers function (f_{14} in the `bbob` suite).

Both objective functions are unimodal and non-separable. The first objective is highly asymmetric in the sense that only one *hypercone* (with angular base area) with a volume of roughly $(1/2)^n$ yields low function values (with the optimum at the tip of the cone). When approaching the second objective's optimum, the sensitivities of the variables in the rotated search space become more and more different.

Contained in the *moderate - ill-conditioned* function group.

Links to illustrations of function F_{23} in dimension 5 for the first instance:

- Search space plot along two coordinate axes
- Projection of the search space into a hyperplane through both optima
- Normalized objective space plot (in log-scale)
- Unscaled objective space plot

8.1.24 F_{24}: Attractive sector/Rastrigin

Combination of the attractive sector function (f_6 in the `bbob` suite) and the Rastrigin function (f_{15} in the `bbob` suite).

Both objectives are non-separable, and the second one is highly multi-modal (roughly 10^n local optima) while the first one is unimodal. Further properties are that the first objective is highly asymmetric and the second has a conditioning of about 10.

Contained in the *moderate - multi-modal* function group.

Links to illustrations of function F_{24} in dimension 5 for the first instance:

- Search space plot along two coordinate axes
- Projection of the search space into a hyperplane through both optima
- Normalized objective space plot (in log-scale)
- Unscaled objective space plot

8.1.25 F_{25}: Attractive sector/Schaffer F7, condition 10

Combination of the attractive sector function (f_6 in the `bbob` suite) and the Schaffer F7 function with condition number 10 (f_{17} in the `bbob` suite).

Both objectives are non-separable and asymmetric. While the first objective is unimodal, the second one is a highly multi-modal function with a low conditioning where frequency and amplitude of the modulation vary.

Contained in the *moderate - multi-modal* function group.

Links to illustrations of function F_{25} in dimension 5 for the first instance:

- Search space plot along two coordinate axes
- Projection of the search space into a hyperplane through both optima
- Normalized objective space plot (in log-scale)
- Unscaled objective space plot

8.1.26 F_{26}: Attractive sector/Schwefel x*sin(x)

Combination of the attractive sector function (f_6 in the `bbob` suite) and the Schwefel function (f_{20} in the `bbob` suite).

The first objective is non-separable, unimodal, and asymmetric. The second objective is partially separable and highly multimodal—having the most prominent 2^n minima located comparatively close to the corners of the unpenalized search area.

Contained in the *moderate - weakly-structured* function group.

Links to illustrations of function F_{26} in dimension 5 for the first instance:

- Search space plot along two coordinate axes
- Projection of the search space into a hyperplane through both optima
- Normalized objective space plot (in log-scale)
- Unscaled objective space plot

8.1.27 F_{27}: Attractive sector/Gallagher 101 peaks

Combination of the attractive sector function (f_6 in the `bbob` suite) and the Gallagher function with 101 peaks (f_{21} in the `bbob` suite).

Both objective functions are non-separable but only the first is unimodal. The first objective function is furthermore asymmetric. The second objective function has 101 optima with position and height being unrelated and randomly chosen (different for each instantiation of the function). The conditioning around the global optimum of the second objective function is about 30.

Contained in the *moderate - weakly-structured* function group.

Links to illustrations of function F_{27} in dimension 5 for the first instance:

- Search space plot along two coordinate axes
- Projection of the search space into a hyperplane through both optima
- Normalized objective space plot (in log-scale)
- Unscaled objective space plot

8.1.28 F_{28}: Rosenbrock original/Rosenbrock original

Combination of two Rosenbrock functions (f_8 in the `bbob` suite).

Both objectives are partially separable (tri-band structure) and have a local optimum with an attraction volume of about 25%.

Contained in the *moderate - moderate* function group.

Links to illustrations of function F_{28} in dimension 5 for the first instance:

- Search space plot along two coordinate axes
- Projection of the search space into a hyperplane through both optima
- Normalized objective space plot (in log-scale)
- Unscaled objective space plot

8.1.29 F_{29}: Rosenbrock original/Sharp ridge

Combination of the Rosenbrock function (f_8 in the `bbob` suite) and the sharp ridge function (f_{13} in the `bbob` suite).

The first objective function is partially separable (tri-band structure) and has a local optimum with an attraction volume of about 25%. The second objective is unimodal and non-separable and, for optimizing it, a sharp, i.e., non-differentiable ridge has to be followed.

Contained in the *moderate - ill-conditioned* function group.

Links to illustrations of function F_{29} in dimension 5 for the first instance:

- Search space plot along two coordinate axes
- Projection of the search space into a hyperplane through both optima
- Normalized objective space plot (in log-scale)
- Unscaled objective space plot

8.1.30 F_{30}: Rosenbrock original/Sum of Different Powers

Combination of the Rosenbrock function (f_8 in the `bbob` suite) and the sum of different powers function (f_{14} in the `bbob` suite).

The first objective function is partially separable (tri-band structure) and has a local optimum with an attraction volume of about 25%. The second objective function is unimodal and non-separable. When approaching the second objective's optimum, the sensitivities of the variables in the rotated search space become more and more different.

Contained in the *moderate - ill-conditioned* function group.

Links to illustrations of function F_{30} in dimension 5 for the first instance:

- Search space plot along two coordinate axes
- Projection of the search space into a hyperplane through both optima
- Normalized objective space plot (in log-scale)
- Unscaled objective space plot

8.1.31 F_{31}: Rosenbrock original/Rastrigin

Combination of the Rosenbrock function (f_8 in the `bbob` suite) and the Rastrigin function (f_{15} in the `bbob` suite).

The first objective function is partially separable (tri-band structure) and has a local optimum with an attraction volume of about 25%. The second objective function is non-separable and highly multi-modal (roughly 10^n local optima).

Contained in the *moderate - multi-modal* function group.

Links to illustrations of function F_{31} in dimension 5 for the first instance:

- Search space plot along two coordinate axes
- Projection of the search space into a hyperplane through both optima
- Normalized objective space plot (in log-scale)
- Unscaled objective space plot

8.1.32 F_{32}: Rosenbrock original/Schaffer F7, condition 10

Combination of the Rosenbrock function (f_8 in the `bbob` suite) and the Schaffer F7 function with condition number 10 (f_{17} in the `bbob` suite).

The first objective function is partially separable (tri-band structure) and has a local optimum with an attraction volume of about 25%. The second objective function is non-separable, asymmetric, and highly multi-modal with a low conditioning where frequency and amplitude of the modulation vary.

Contained in the *moderate - multi-modal* function group.

Links to illustrations of function F_{32} in dimension 5 for the first instance:

- Search space plot along two coordinate axes
- Projection of the search space into a hyperplane through both optima
- Normalized objective space plot (in log-scale)
- Unscaled objective space plot

8.1.33 F_{33}: Rosenbrock original/Schwefel x*sin(x)

Combination of the Rosenbrock function (f_8 in the `bbob` suite) and the Schwefel function (f_{20} in the `bbob` suite).

Both objective functions are partially separable. While the first objective function has a local optimum with an attraction volume of about 25%, the second objective function is highly multimodal—having the most prominent 2^n minima located comparatively close to the corners of its unpenalized search area.

Contained in the *moderate - weakly-structured* function group.

Links to illustrations of function F_{33} in dimension 5 for the first instance:

- Search space plot along two coordinate axes
- Projection of the search space into a hyperplane through both optima
- Normalized objective space plot (in log-scale)
- Unscaled objective space plot

8.1.34 F_{34}: Rosenbrock original/Gallagher 101 peaks

Combination of the Rosenbrock function (f_8 in the `bbob` suite) and the Gallagher function with 101 peaks (f_{21} in the `bbob` suite).

The first objective function is partially separable, the second one non-separable. While the first objective function has a local optimum with an attraction volume of about 25%, the second objective function has 101 optima with position and height being unrelated and randomly chosen (different for each instantiation of the function). The conditioning around the global optimum of the second objective function is about 30.

Contained in the *moderate - weakly-structured* function group.

Links to illustrations of function F_{34} in dimension 5 for the first instance:

- Search space plot along two coordinate axes
- Projection of the search space into a hyperplane through both optima
- Normalized objective space plot (in log-scale)
- Unscaled objective space plot

8.1.35 F_{35}: Sharp ridge/Sharp ridge

Combination of two sharp ridge functions (f_{13} in the `bbob` suite).

Both objective functions are unimodal and non-separable and, for optimizing them, two sharp, i.e., non-differentiable ridges have to be followed.

Contained in the *ill-conditioned - ill-conditioned* function group.

Links to illustrations of function F_{35} in dimension 5 for the first instance:

- Search space plot along two coordinate axes
- Projection of the search space into a hyperplane through both optima
- Normalized objective space plot (in log-scale)
- Unscaled objective space plot

8.1.36 F_{36}: Sharp ridge/Sum of Different Powers

Combination of the sharp ridge function (f_{13} in the `bbob` suite) and the sum of different powers function (f_{14} in the `bbob` suite).

Both functions are uni-modal and non-separable. For optimizing the first objective, a sharp, i.e., non-differentiable ridge has to be followed. When approaching the second objective's optimum, the sensitivities of the variables in the rotated search space become more and more different.

Contained in the *ill-conditioned - ill-conditioned* function group.

Links to illustrations of function F_{36} in dimension 5 for the first instance:

- Search space plot along two coordinate axes
- Projection of the search space into a hyperplane through both optima
- Normalized objective space plot (in log-scale)
- Unscaled objective space plot

8.1.37 F_{37}: Sharp ridge/Rastrigin

Combination of the sharp ridge function (f_{13} in the `bbob` suite) and the Rastrigin function (f_{15} in the `bbob` suite).

Both functions are non-separable. While the first one is unimodal and non-differentiable at its ridge, the second objective function is highly multi-modal (roughly 10^n local optima).

Contained in the *ill-conditioned - multi-modal* function group.

Links to illustrations of function F_{37} in dimension 5 for the first instance:

- Search space plot along two coordinate axes
- Projection of the search space into a hyperplane through both optima
- Normalized objective space plot (in log-scale)
- Unscaled objective space plot

8.1.38 F_{38}: Sharp ridge/Schaffer F7, condition 10

Combination of the sharp ridge function (f_{13} in the `bbob` suite) and the Schaffer F7 function with condition number 10 (f_{17} in the `bbob` suite).

Both functions are non-separable. While the first one is unimodal and non-differentiable at its ridge, the second objective function is asymmetric and highly multi-modal with a low conditioning where frequency and amplitude of the modulation vary.

Contained in the *ill-conditioned - multi-modal* function group.

Links to illustrations of function F_{38} in dimension 5 for the first instance:

- Search space plot along two coordinate axes
- Projection of the search space into a hyperplane through both optima
- Normalized objective space plot (in log-scale)
- Unscaled objective space plot

8.1.39 F_{39}: Sharp ridge/Schwefel x*sin(x)

Combination of the sharp ridge function (f_{13} in the `bbob` suite) and the Schwefel function (f_{20} in the `bbob` suite).

While the first objective function is unimodal, non-separable, and non-differentiable at its ridge, the second objective function is highly multimodal—having the most prominent 2^n minima located comparatively close to the corners of its unpenalized search area.

Contained in the *ill-conditioned - weakly-structured* function group.

Links to illustrations of function F_{39} in dimension 5 for the first instance:

- Search space plot along two coordinate axes
- Projection of the search space into a hyperplane through both optima
- Normalized objective space plot (in log-scale)
- Unscaled objective space plot

8.1.40 F_{40}: Sharp ridge/Gallagher 101 peaks

Combination of the sharp ridge function (f_{13} in the `bbob` suite) and the Gallagher function with 101 peaks (f_{21} in the `bbob` suite).

Both objective functions are non-separable. While the first objective function is unimodal and non-differentiable at its ridge, the second objective function has 101 optima with position and height being unrelated and randomly chosen (different for each instantiation of the function). The conditioning around the global optimum of the second objective function is about 30.

Contained in the *ill-conditioned - weakly-structured* function group.

Links to illustrations of function F_{40} in dimension 5 for the first instance:

- Search space plot along two coordinate axes
- Projection of the search space into a hyperplane through both optima
- Normalized objective space plot (in log-scale)
- Unscaled objective space plot

8.1.41 F_{41}: Sum of Different Powers/Sum of Different Powers

Combination of two sum of different powers functions (f_{14} in the `bbob` suite).

Both functions are uni-modal and non-separable where the sensitivities of the variables in the rotated search space become more and more different when approaching the objectives' optima.

Contained in the *ill-conditioned - ill-conditioned* function group.

Links to illustrations of function F_{41} in dimension 5 for the first instance:

- Search space plot along two coordinate axes
- Projection of the search space into a hyperplane through both optima
- Normalized objective space plot (in log-scale)
- Unscaled objective space plot

8.1.42 F_{42}: Sum of Different Powers/Rastrigin

Combination of the sum of different powers functions (f_{14} in the `bbob` suite) and the Rastrigin function (f_{15} in the `bbob` suite).

Both objective functions are non-separable. While the first one is unimodal, the second objective function is highly multi-modal (roughly 10^n local optima).

Contained in the *ill-conditioned - multi-modal* function group.

Links to illustrations of function F_{42} in dimension 5 for the first instance:

- Search space plot along two coordinate axes
- Projection of the search space into a hyperplane through both optima
- Normalized objective space plot (in log-scale)
- Unscaled objective space plot

8.1.43 F_{43}: Sum of Different Powers/Schaffer F7, condition 10

Combination of the sum of different powers functions (f_{14} in the `bbob` suite) and the Schaffer F7 function with condition number 10 (f_{17} in the `bbob` suite).

Both objective functions are non-separable. While the first one is unimodal with an increasing conditioning once the optimum is approached, the second objective function is asymmetric and highly multi-modal with a low conditioning where frequency and amplitude of the modulation vary.

Contained in the *ill-conditioned - multi-modal* function group.

Links to illustrations of function F_{43} in dimension 5 for the first instance:

- Search space plot along two coordinate axes
- Projection of the search space into a hyperplane through both optima
- Normalized objective space plot (in log-scale)
- Unscaled objective space plot

8.1.44 F_{44}: Sum of Different Powers/Schwefel x*sin(x)

Combination of the sum of different powers functions (f_{14} in the `bbob` suite) and the Schwefel function (f_{20} in the `bbob` suite).

Both objectives are non-separable. While the first objective function is unimodal, the second objective function is highly multimodal—having the most prominent 2^n minima located comparatively close to the corners of its unpenalized search area.

Contained in the *ill-conditioned - weakly-structured* function group.

Links to illustrations of function F_{44} in dimension 5 for the first instance:

- Search space plot along two coordinate axes
- Projection of the search space into a hyperplane through both optima
- Normalized objective space plot (in log-scale)
- Unscaled objective space plot

8.1.45 F_{45}: Sum of Different Powers/Gallagher 101 peaks

Combination of the sum of different powers functions (f_{14} in the `bbob` suite) and the Gallagher function with 101 peaks (f_{21} in the `bbob` suite).

Both objective functions are non-separable. While the first objective function is unimodal, the second objective function has 101 optima with position and height being unrelated and randomly chosen (different for each instantiation of the function). The conditioning around the global optimum of the second objective function is about 30.

Contained in the *ill-conditioned - weakly-structured* function group.

Links to illustrations of function F_{45} in dimension 5 for the first instance:

- Search space plot along two coordinate axes
- Projection of the search space into a hyperplane through both optima
- Normalized objective space plot (in log-scale)
- Unscaled objective space plot

8.1.46 F_{46}: Rastrigin/Rastrigin

Combination of two Rastrigin functions (f_{15} in the `bbob` suite).

Both objective functions are non-separable and highly multi-modal (roughly 10^n local optima).

Contained in the *multi-modal - multi-modal* function group.

Links to illustrations of function F_{46} in dimension 5 for the first instance:

- Search space plot along two coordinate axes
- Projection of the search space into a hyperplane through both optima
- Normalized objective space plot (in log-scale)
- Unscaled objective space plot

8.1.47 F_{47}: Rastrigin/Schaffer F7, condition 10

Combination of the Rastrigin function (f_{15} in the `bbob` suite) and the Schaffer F7 function with condition number 10 (f_{17} in the `bbob` suite).

Both objective functions are non-separable and highly multi-modal.

Contained in the *multi-modal - multi-modal* function group.

Links to illustrations of function F_{47} in dimension 5 for the first instance:

- Search space plot along two coordinate axes
- Projection of the search space into a hyperplane through both optima
- Normalized objective space plot (in log-scale)
- Unscaled objective space plot

8.1.48 F_{48}: Rastrigin/Schwefel x*sin(x)

Combination of the Rastrigin function (f_{15} in the `bbob` suite) and the Schwefel function (f_{20} in the `bbob` suite).

Both objective functions are non-separable and highly multi-modal where the first has roughly 10^n local optima and the most prominent 2^n minima of the second objective function are located comparatively close to the corners of its unpenalized search area.

Contained in the *multi-modal - weakly-structured* function group.

Links to illustrations of function F_{48} in dimension 5 for the first instance:

- Search space plot along two coordinate axes
- Projection of the search space into a hyperplane through both optima
- Normalized objective space plot (in log-scale)
- Unscaled objective space plot

8.1.49 F_{49}: Rastrigin/Gallagher 101 peaks

Combination of the Rastrigin function (f_{15} in the `bbob` suite) and the Gallagher function with 101 peaks (f_{21} in the `bbob` suite).

Both objective functions are non-separable and highly multi-modal where the first has roughly 10^n local optima and the second has 101 optima with position and height being unrelated and randomly chosen (different for each instantiation of the function).

Contained in the *multi-modal - weakly-structured* function group.

Links to illustrations of function F_{49} in dimension 5 for the first instance:

- Search space plot along two coordinate axes
- Projection of the search space into a hyperplane through both optima
- Normalized objective space plot (in log-scale)
- Unscaled objective space plot

8.1.50 F_{50}: Schaffer F7, condition 10/Schaffer F7, condition 10

Combination of two Schaffer F7 functions with condition number 10 (f_{17} in the `bbob` suite).

Both objective functions are non-separable and highly multi-modal.
Contained in the *multi-modal - multi-modal* function group.

Links to illustrations of function F_{50} in dimension 5 for the first instance:

- Search space plot along two coordinate axes
- Projection of the search space into a hyperplane through both optima
- Normalized objective space plot (in log-scale)
- Unscaled objective space plot

8.1.51 F_{51}: Schaffer F7, condition 10/Schwefel x*sin(x)

Combination of the Schaffer F7 function with condition number 10 (f_{17} in the `bbob` suite) and the Schwefel function (f_{20} in the `bbob` suite).

Both objective functions are non-separable and highly multi-modal. While frequency and amplitude of the modulation vary in an almost regular fashion in the first objective function, the second objective function possesses less global structure.

Contained in the *multi-modal - weakly-structured* function group.

Links to illustrations of function F_{51} in dimension 5 for the first instance:

- Search space plot along two coordinate axes
- Projection of the search space into a hyperplane through both optima
- Normalized objective space plot (in log-scale)
- Unscaled objective space plot

8.1.52 F_{52}: Schaffer F7, condition 10/Gallagher 101 peaks

Combination of the Schaffer F7 function with condition number 10 (f_{17} in the `bbob` suite) and the Gallagher function with 101 peaks (f_{21} in the `bbob` suite).

Both objective functions are non-separable and highly multi-modal. While frequency and amplitude of the modulation vary in an almost regular fashion in the first objective function, the second has 101 optima with position and height being unrelated and randomly chosen (different for each instantiation of the function).

Contained in the *multi-modal - weakly-structured* function group.

Links to illustrations of function F_{52} in dimension 5 for the first instance:

- Search space plot along two coordinate axes
- Projection of the search space into a hyperplane through both optima
- Normalized objective space plot (in log-scale)
- Unscaled objective space plot

8.1.53 F_{53}: Schwefel x*sin(x)/Schwefel x*sin(x)

Combination of two Schwefel functions (f_{20} in the `bbob` suite).

Both objective functions are non-separable and highly multi-modal where the most prominent 2^n minima of each objective function are located comparatively close to the corners of its unpenalized search area. Due to the combinatorial nature of the Schwefel function, it is likely in low dimensions that the Pareto set goes through the origin of the search space.

Contained in the *weakly-structured - weakly-structured* function group.

Links to illustrations of function F_{53} in dimension 5 for the first instance:

- Search space plot along two coordinate axes
- Projection of the search space into a hyperplane through both optima
- Normalized objective space plot (in log-scale)
- Unscaled objective space plot

8.1.54 F_{54}: Schwefel x*sin(x)/Gallagher 101 peaks

Combination of the Schwefel function (f_{20} in the `bbob` suite) and the Gallagher function with 101 peaks (f_{21} in the `bbob` suite).

Both objective functions are non-separable and highly multi-modal. For the first objective function, the most prominent 2^n minima are located comparatively close to the corners of its unpenalized search area. For the second objective, position and height of all 101 optima are unrelated and randomly chosen (different for each instantiation of the function).

Contained in the *weakly-structured - weakly-structured* function group.

Links to illustrations of function F_{54} in dimension 5 for the first instance:

- Search space plot along two coordinate axes
- Projection of the search space into a hyperplane through both optima
- Normalized objective space plot (in log-scale)
- Unscaled objective space plot

8.1.55 F_{55}: Gallagher 101 peaks/Gallagher 101 peaks

Combination of two Gallagher functions with 101 peaks (f_{21} in the `bbob` suite).

Both objective functions are non-separable and highly multi-modal. Position and height of all 101 optima in each objective function are unrelated and randomly chosen and thus, no global structure is present.

Contained in the *weakly-structured - weakly-structured* function group.

Links to illustrations of function F_{55} in dimension 5 for the first instance:

- Search space plot along two coordinate axes
- Projection of the search space into a hyperplane through both optima
- Normalized objective space plot (in log-scale)
- Unscaled objective space plot

8.1.56 F_{56}: Sphere/Rastrigin separable

Combination of the Sphere function (f_1 in the `bbob` suite) and the separable Rastrigin function (f_3 in the `bbob` suite).

While the first objective function is unimodal, highly symmetric, rotational and scale invariant, the second one is highly multimodal with a comparatively regular structure for the placement of the optima. Note that the non-linear transformations of the second objective's Rastrigin function alleviate the symmetry and regularity of the original Rastrigin function.

Contained in the *separable - separable* function group.

Links to illustrations of function F_{56} in dimension 5 for the first instance:

- Search space plot along two coordinate axes
- Projection of the search space into a hyperplane through both optima
- Normalized objective space plot (in log-scale)
- Unscaled objective space plot

8.1.57 F_{57}: Sphere/Rastrigin-Büche

Combination of the Sphere function (f_1 in the `bbob` suite) and the separable Büche-Rastrigin function (f_4 in the `bbob` suite).

While the first objective function is unimodal, highly symmetric, rotational and scale invariant, the second one is highly multimodal with a structured but highly asymmetric placement of the optima. Constructed as a deceptive function for symmetrically distributed search operators, the second objective function has roughly 10D local optima, a conditioning of about 10, and a skew factor of about 10 in x-space and 100 in f-space.

Contained in the *separable - separable* function group.

Links to illustrations of function F_{57} in dimension 5 for the first instance:

- Search space plot along two coordinate axes
- Projection of the search space into a hyperplane through both optima
- Normalized objective space plot (in log-scale)
- Unscaled objective space plot

8.1.58 F_{58}: Sphere/Linear slope

Combination of the Sphere function (f_1 in the `bbob` suite) and the Linear Slope function (f_5 in the `bbob` suite).

Both objective functions are separable and amongst the simplest continuous functions to optimize. The first objective function is fully quadratic and symmetric around the optimum, the second objective function is fully linear within the hypercube $[-5, 5]^n$ and has a region of constant f-value outside the hypercube by definition to ensure that a solution at one corner of $[-5, 5]^n$ has optimal function value.

Contained in the *separable - separable* function group.

Links to illustrations of function F_{58} in dimension 5 for the first instance:

- Search space plot along two coordinate axes
- Projection of the search space into a hyperplane through both optima
- Normalized objective space plot (in log-scale)
- Unscaled objective space plot

8.1.59 F_{59}: Separable Ellipsoid/Separable Rastrigin

Combination of the separable Ellipsoid function (f_2 in the `bbob` suite) and the separable Rastrigin function (f_3 in the `bbob` suite).

Besides being both separable, the two objective functions are quite opposite: the first objective function is unimodal, globally quadratic and ill-conditioned with a conditioning of about 10^6 with smooth local irregularities while the second objective function is highly multimodal with roughly $10n$ local optima and only small conditioning of about 10. Note that the separable Rastrigin function has a comparatively regular structure for the placement of the optima but asymmetric and oscillating non-linear transformations of this function alleviates the symmetry and regularity of the original Rastrigin function.

Contained in the *separable - separable* function group.

Links to illustrations of function F_{59} in dimension 5 for the first instance:

- Search space plot along two coordinate axes
- Projection of the search space into a hyperplane through both optima
- Normalized objective space plot (in log-scale)
- Unscaled objective space plot

8.1.60 F_{60}: separable Ellipsoid/Büche-Rastrigin

Combination of the separable Ellipsoid function (f_2 in the `bbob` suite) and the separable Büche-Rastrigin function (f_4 in the `bbob` suite).

Besides being both separable, the two objective functions are quite opposite: the first objective function is unimodal, globally quadratic and ill-conditioned with a conditioning of about 10^6 with smooth local irregularities while the second objective is highly multimodal with a structured but highly asymmetric placement of the optima. Constructed as a deceptive function for symmetrically distributed search operators.

Contained in the *separable - separable* function group.

Links to illustrations of function F_{60} in dimension 5 for the first instance:

- Search space plot along two coordinate axes
- Projection of the search space into a hyperplane through both optima
- Normalized objective space plot (in log-scale)
- Unscaled objective space plot

8.1.61 F_{61}: Separable Ellipsoid/Linear Slope

Combination of the separable Ellipsoid function (f_2 in the `bbob` suite) and the Linear Slope function (f_5 in the `bbob` suite).

Both objective functions are separable. The first objective function is unimodal with a high condition number of about 10^6. The second objective function is fully linear within the hypercube $[-5, 5]^n$ and has a region of constant f-value outside the hypercube by definition to ensure that a solution at one corner of $[-5, 5]^n$ has optimal function value.

Contained in the *separable - separable* function group.

Links to illustrations of function F_{61} in dimension 5 for the first instance:

- Search space plot along two coordinate axes
- Projection of the search space into a hyperplane through both optima
- Normalized objective space plot (in log-scale)
- Unscaled objective space plot

8.1.62 F_{62}: separable Rastrigin/Büche-Rastrigin

Combination of the separable Rastrigin function (f_3 in the `bbob` suite) and the separable Büche-Rastrigin function (f_4 in the `bbob` suite).

Both objective functions are separable and highly multimodal with an underlying structure for the placements of the optima. While for the separable Rastrigin function, the placements of the optima is symmetric, the optima for the Büche-Rastrigin function are highly asymmetrically placed.

Contained in the *separable - separable* function group.

Links to illustrations of function F_{62} in dimension 5 for the first instance:

- Search space plot along two coordinate axes
- Projection of the search space into a hyperplane through both optima
- Normalized objective space plot (in log-scale)
- Unscaled objective space plot

8.1.63 F_{63}: Separable Rastrigin/Linear Slope

Combination of the separable Rastrigin function (f_3 in the `bbob` suite) and the Linear Slope function (f_5 in the `bbob` suite).

Both objective functions are separable, but while the first objective function is highly multi-modal with an underlying symmetric structure, the second objective function is purely linear with plateaus of constant function value outside the region $[-5, 5]^n$.

Contained in the *separable - separable* function group.

Links to illustrations of function F_{63} in dimension 5 for the first instance:

- Search space plot along two coordinate axes
- Projection of the search space into a hyperplane through both optima
- Normalized objective space plot (in log-scale)
- Unscaled objective space plot

8.1.64 F_{64}: Büche-Rastrigin/Linear slope

Combination of the Büche-Rastrigin function (f_4 in the `bbob` suite) and the Linear Slope function (f_5 in the `bbob` suite).

Both objective functions are separable, but while the first objective function is highly multi-modal with an underlying asymmetric structure, the second objective function is purely linear with plateaus of constant function value outside the region $[-5, 5]^n$.

Contained in the *separable - separable* function group.

Links to illustrations of function F_{64} in dimension 5 for the first instance:

- Search space plot along two coordinate axes
- Projection of the search space into a hyperplane through both optima
- Normalized objective space plot (in log-scale)
- Unscaled objective space plot

8.1.65 F_{65}: Attractive Sector/Step-ellipsoid

Combination of the Attractive Sector function (f_6 in the `bbob` suite) and the Step Ellipsoidal function (f_7 in the `bbob` suite).

Both objective functions are unimodal and of moderate conditioning. The first objective function is highly asymmetric, where only one *hypercone* (with angular base area) with a volume of roughly $1/2^n$ yields low function values. The optimum of the first objective is located at the tip of this cone. This function can be deceptive for cumulative step size adaptation. The second objective function consists of many plateaus of different sizes. Apart from a small area close to the global optimum, the gradient is zero almost everywhere.

Contained in the *moderate - moderate* function group.

Links to illustrations of function F_{65} in dimension 5 for the first instance:

- Search space plot along two coordinate axes
- Projection of the search space into a hyperplane through both optima
- Normalized objective space plot (in log-scale)
- Unscaled objective space plot

8.1.66 F_{66}: Attractive Sector/rotated Rosenbrock

Combination of the Attractive Sector function (f_6 in the `bbob` suite) and the rotated Rosenbrock function (f_9 in the `bbob` suite).

The first objective function is highly asymmetric, where only one *hypercone* (with angular base area) with a volume of roughly $1/2^n$ yields low function values. The optimum of the first objective is located at the tip of this cone. The second objective function is the so-called banana function due to its 2-D contour lines as a bent ridge (or valley) and partially separable (tri-band structure). In larger dimensions, the second objective function has a local optimum with an attraction volume of about 25%. Note that, compared to the original Rosenbrock function, a rotation in the search space is applied, such that the second objective function is non-separable.

Contained in the *moderate - moderate* function group.

Links to illustrations of function F_{66} in dimension 5 for the first instance:

- Search space plot along two coordinate axes
- Projection of the search space into a hyperplane through both optima
- Normalized objective space plot (in log-scale)
- Unscaled objective space plot

8.1.67 F_{67}: Step-ellipsoid/separable Rosenbrock

Combination of the Step Ellipsoidal function (f_7 in the `bbob` suite) and the separable Rosenbrock function (f_8 in the `bbob` suite).

The first objective function is unimodal, non-separable, and has a conditioning of about 100. It actually consists of many plateaus of different sizes. Apart from a small area close to the global optimum, the gradient is zero almost everywhere. The second objective function is the so-called banana function due to its 2-D contour lines as a bent ridge (or valley). It is partially separable (tri-band structure) and in larger dimensions, the function has a local optimum with an attraction volume of about 25%.

Contained in the *moderate - moderate* function group.

Links to illustrations of function F_{67} in dimension 5 for the first instance:

- Search space plot along two coordinate axes
- Projection of the search space into a hyperplane through both optima
- Normalized objective space plot (in log-scale)
- Unscaled objective space plot

8.1.68 F_{68}: Step-ellipsoid/rotated Rosenbrock

Combination of the Step Ellipsoidal function (f_7 in the `bbob` suite) and the rotated Rosenbrock function (f_9 in the `bbob` suite).

The first objective function is unimodal, non-separable, and has a conditioning of about 100. It actually consists of many plateaus of different sizes. Apart from a small area close to the global optimum, the gradient is zero almost everywhere. The second objective function is a rotated version of the original so-called banana function (due to its 2-D contour lines as a bent ridge or valley) and in larger dimensions, has a local optimum with an attraction volume of about 25%.

This function resembles F_{67} except for the additional search space rotation for the second objective function which makes both objective function fully non-separable.

Contained in the *moderate - moderate* function group.

Links to illustrations of function F_{68} in dimension 5 for the first instance:

- Search space plot along two coordinate axes
- Projection of the search space into a hyperplane through both optima
- Normalized objective space plot (in log-scale)
- Unscaled objective space plot

8.1.69 F_{69}: separable Rosenbrock/rotated Rosenbrock

Combination of the separable Rosenbrock function (f_8 in the `bbob` suite) and the rotated Rosenbrock function (f_9 in the `bbob` suite).

Both objective functions are Rosenbrock functions (also known under the name banana function due to its 2-D contour lines forming a bent ridge or valley) with a local optimum in large dimension that has about 25% attraction volume. The first objective function is partially separable while the second objective function is fully non-separable.

Contained in the *moderate - moderate* function group.

Links to illustrations of function F_{69} in dimension 5 for the first instance:

- Search space plot along two coordinate axes
- Projection of the search space into a hyperplane through both optima
- Normalized objective space plot (in log-scale)
- Unscaled objective space plot

8.1.70 F_{70}: Ellipsoid/Discus

Combination of the Ellipsoid function (f_{10} in the `bbob` suite) and the Discus (or Tablet) function (f_{11} in the `bbob` suite).

Both objective functions are globally quadratic (unimodal) ill-conditioned functions with condition numbers of 10^6 with smooth local irregularities. A single direction in search space is a thousand times more sensitive than all others for the Discus function.

Contained in the *ill-conditioned - ill-conditioned* function group.

Links to illustrations of function F_{70} in dimension 5 for the first instance:

- Search space plot along two coordinate axes
- Projection of the search space into a hyperplane through both optima
- Normalized objective space plot (in log-scale)
- Unscaled objective space plot

8.1.71 F_{71}: Ellipsoid/Bent Cigar

Combination of the Ellipsoid function (f_{10} in the `bbob` suite) and the Bent Cigar function (f_{12} in the `bbob` suite).

Both objective functions are unimodal, non-separable, and have a conditioning of about 10^6. The Ellipsoid function is globally quadratic with smooth local irregularities while the Bent Cigar function deviates remarkably from being quadratic due to an asymmetric transformation. To optimize the Bent Cigar function, a smooth, but very narrow ridge has to be followed.

Contained in the *ill-conditioned - ill-conditioned* function group.

Links to illustrations of function F_{71} in dimension 5 for the first instance:

- Search space plot along two coordinate axes
- Projection of the search space into a hyperplane through both optima
- Normalized objective space plot (in log-scale)
- Unscaled objective space plot

8.1.72 F_{72}: Ellipsoid/Sharp Ridge

Combination of the Ellipsoid function (f_{10} in the `bbob` suite) and the Sharp Ridge function (f_{13} in the `bbob` suite).

Both objective functions are unimodal, non-separable, and have a conditioning of about 10^6. Compared to the previous function, the ridge of the here is sharp (non-differentiable) and the gradient remains constant, when the ridge is approached from a given point. Approaching the ridge is initially effective, but search behavior becomes difficult to diagnose close to the ridge because the gradient towards the ridge does not flatten out.

Contained in the *ill-conditioned - ill-conditioned* function group.

Links to illustrations of function F_{72} in dimension 5 for the first instance:

- Search space plot along two coordinate axes
- Projection of the search space into a hyperplane through both optima
- Normalized objective space plot (in log-scale)
- Unscaled objective space plot

8.1.73 F_{73}: Ellipsoid/Sum of Different Powers

Combination of the Ellipsoid function (f_{10} in the `bbob` suite) and the Sum of Different Powers function (f_{14} in the `bbob` suite).

Both objective functions are unimodal and non-separable. While the Ellipsoid function has a constant conditioning of 10^6 everywhere, the sensitivities of the z_i-variables (in the rotated search space) for the Different Powers function become more and more different when approaching the optimum. The latter function has furthermore a small solution volume.

Contained in the *ill-conditioned - ill-conditioned* function group.

Links to illustrations of function F_{73} in dimension 5 for the first instance:

- Search space plot along two coordinate axes
- Projection of the search space into a hyperplane through both optima
- Normalized objective space plot (in log-scale)
- Unscaled objective space plot

8.1.74 F_{74}: Discus/Bent Cigar

Combination of the Discus function (f_{11} in the `bbob` suite) and the Bent cigar function (f_{12} in the `bbob` suite).

Both objective functions are unimodal, non-separable, and have a conditioning of about 10^6. The Discus function is globally quadratic with smooth local irregularities and has a single direction in search space that is a thousand times more sensitive than all others. The Bent Cigar function deviates remarkably from being quadratic due to an asymmetric transformation and a smooth, but very narrow ridge has to be followed to optimize it.

Contained in the *ill-conditioned - ill-conditioned* function group.

Links to illustrations of function F_{74} in dimension 5 for the first instance:

- Search space plot along two coordinate axes
- Projection of the search space into a hyperplane through both optima
- Normalized objective space plot (in log-scale)
- Unscaled objective space plot

8.1.75 F_{75}: Discus/Sharp Ridge

Combination of the Discus function (f_{11} in the `bbob` suite) and the Sharp Ridge function (f_{13} in the `bbob` suite).

Both objective functions are unimodal, non-separable, and have a conditioning of about 10^6. The Discus function is globally quadratic with smooth local irregularities and has a single direction in search space that is a thousand times more sensitive than all others. To optimize the Sharp Ridge function, a sharp (i.e. non-differentiable) ridge has to be followed around which the gradient remains constant, when the ridge is approached from a given point. Approaching the ridge is initially effective, but search behavior becomes difficult to diagnose close to the ridge because the gradient towards the ridge does not flatten out.

Contained in the *ill-conditioned - ill-conditioned* function group.

Links to illustrations of function F_{75} in dimension 5 for the first instance:

- Search space plot along two coordinate axes
- Projection of the search space into a hyperplane through both optima
- Normalized objective space plot (in log-scale)
- Unscaled objective space plot

8.1.76 F_{76}: Discus/Sum of Different Powers

Combination of the Discus function (f_{11} in the `bbob` suite) and the Sum of Different Powers function (f_{14} in the `bbob` suite).

Both objective functions are unimodal and non-separable. While the globally quadratic Discus function has a constant conditioning of about 10^6 everywhere with a single direction in search space that is a thousand times more sensitive than all others, the sensitivities of the z_i-variables (in the rotated search space) for the Different Powers function become more and more different when approaching the optimum. The latter function has furthermore a small solution volume.

Contained in the *ill-conditioned - ill-conditioned* function group.

Links to illustrations of function F_{76} in dimension 5 for the first instance:

- Search space plot along two coordinate axes
- Projection of the search space into a hyperplane through both optima
- Normalized objective space plot (in log-scale)
- Unscaled objective space plot

8.1.77 F_{77}: Bent Cigar/Sharp Ridge

Combination of the Bent Cigar function (f_{12} in the `bbob` suite) and the Sharp Ridge function (f_{13} in the `bbob` suite).

Both objective functions are unimodal, non-separable, and have a conditioning of about 10^6. The Bent Cigar function deviates remarkably from being quadratic due to an asymmetric transformation and a smooth, but very narrow ridge has to be followed to optimize it. To optimize the Sharp Ridge function, in turn, the ridge to be followed is even sharper (i.e. non-differentiable), around which the gradient remains constant, when the ridge is approached from a given point. Approaching the ridge is initially effective, but search behavior becomes difficult to diagnose close to the ridge because the gradient towards the ridge does not flatten out.

Contained in the *ill-conditioned - ill-conditioned* function group.

Links to illustrations of function F_{77} in dimension 5 for the first instance:

- Search space plot along two coordinate axes
- Projection of the search space into a hyperplane through both optima
- Normalized objective space plot (in log-scale)
- Unscaled objective space plot

8.1.78 F_{78}: Bent Cigar/Sum of Different Powers

Combination of the Bent Cigar function (f_{12} in the `bbob` suite) and the Sum of Different Powers function (f_{14} in the `bbob` suite).

Both objective functions are unimodal, non-separable, and have a conditioning of about 10^6.

Both objective functions are unimodal and non-separable but differ in the difficulties provided to an optimization algorithm. The Bent Cigar function, on the one hand, deviates remarkably from being quadratic due to an asymmetric transformation and a smooth, but very narrow ridge has to be followed to optimize it. The sensitivities of the z_i-variables (in the rotated search space) for the Different Powers function, on the other hand, become more and more different when approaching the optimum.

Contained in the *ill-conditioned - ill-conditioned* function group.

Links to illustrations of function F_{78} in dimension 5 for the first instance:

- Search space plot along two coordinate axes
- Projection of the search space into a hyperplane through both optima
- Normalized objective space plot (in log-scale)
- Unscaled objective space plot

8.1.79 F_{79}: Rastrigin/Schaffer F7 with conditioning of 1000

Combination of the Rastrigin function (f_{15} in the `bbob` suite) and the Schaffer F7 function with conditioning 1000 (f_{18} in the `bbob` suite).

Both objective functions are non-separable and highly multimodal. The problem's Rastrigin function alleviates the symmetry and regularity of the originally proposed Rastrigin function via asymmetric and oscillating transformations of the search space. It has roughly 10^n local optima, a low conditioning, and the global amplitude of function values is large compared to the local amplitudes. On the contrary, frequency and amplitude of the function value modulation vary for the Schaffer F7 function. It is furthermore asymmetric as well but, compared to the other objective function is moderately ill-conditioned with a conditioning of 1000.

Contained in the *multi-modal - multi-modal* function group.

Links to illustrations of function F_{79} in dimension 5 for the first instance:

- Search space plot along two coordinate axes
- Projection of the search space into a hyperplane through both optima
- Normalized objective space plot (in log-scale)
- Unscaled objective space plot

8.1.80 F_{80}: Rastrigin/Griewank-Rosenbrock

Combination of the Rastrigin function (f_{15} in the `bbob` suite) and the Griewank-Rosenbrock function (f_{19} in the `bbob` suite).

Both objective functions are non-separable and highly multimodal. Both objective functions furthermore are variants of the original Rosenbrock function: The problem's Rastrigin function alleviates the symmetry and regularity of the originally proposed Rastrigin function via asymmetric and oscillating transformations of the search space. The Griewank-Rosenbrock function resembles the original Rosenbrock function in a highly multimodal way.

Contained in the *multi-modal multi-modal* function group.

Links to illustrations of function F_{80} in dimension 5 for the first instance:

- Search space plot along two coordinate axes
- Projection of the search space into a hyperplane through both optima
- Normalized objective space plot (in log-scale)
- Unscaled objective space plot

8.1.81 F_{81}: Schaffer F7/Schaffer F7 with conditioning 1000

Combination of the Schaffer F7 function (f_{17} in the `bbob` suite) and the Schaffer F7 with conditioning 1000 function (f_{18} in the `bbob` suite).

Both objective functions are of the same type (asymmetric, non-separable, highly multimodal where frequency and amplitude of the modulation vary). The main difference is in the conditioning, which is about 10 in one case and 1000 in the other.

Contained in the *multi-modal - multi-modal* function group.

Links to illustrations of function F_{81} in dimension 5 for the first instance:

- Search space plot along two coordinate axes
- Projection of the search space into a hyperplane through both optima
- Normalized objective space plot (in log-scale)
- Unscaled objective space plot

8.1.82 F_{82}: Schaffer F7/Griewank-Rosenbrock

Combination of the Schaffer F7 function (f_{17} in the `bbob` suite) and the Griewank-Rosenbrock function (f_{19} in the `bbob` suite).

Both objective functions are non-separable and highly multimodal. For the asymmetric Schaffer F7 function, frequency and amplitude of the function value modulation vary and it has a low conditioning of about 10. The Griewank-Rosenbrock function resembles the original Rosenbrock function in a highly multimodal way.

Contained in the *multi-modal - multi-modal* function group.

Links to illustrations of function F_{82} in dimension 5 for the first instance:

- Search space plot along two coordinate axes
- Projection of the search space into a hyperplane through both optima
- Normalized objective space plot (in log-scale)
- Unscaled objective space plot

8.1.83 F_{83}: Schaffer F7 with conditioning 1000/Griewank-Rosenbrock

Combination of the Schaffer F7 function with conditioning 1000 (f_{18} in the `bbob` suite) and the Griewank-Rosenbrock function (f_{19} in the `bbob` suite).

Compared to F_{82}, the only difference is the higher condition number of about 1000 (compared to 10) in the Schaffer F7 function.

Contained in the *multi-modal - multi-modal* function group.

Links to illustrations of function F_{83} in dimension 5 for the first instance:

- Search space plot along two coordinate axes
- Projection of the search space into a hyperplane through both optima
- Normalized objective space plot (in log-scale)
- Unscaled objective space plot

8.1.84 F_{84}: Schwefel/Gallagher 21

Combination of the Schwefel function (f_{20} in the `bbob` suite) and the Gallagher 21 function (f_{22} in the `bbob` suite).

Both objective functions are multi-modal with only a weak global structure. The most prominent 2^n minima of the Schwefel function are located comparatively close to the corners of the unpenalized search area. The penalization is essential, as otherwise more and better minima occur further away from the search space origin. The function is furthermore partially separable, a kind of combinatorial problem, and has two search regimes. The Gallagher function consists of 21 optima with position and height being unrelated and randomly chosen (different for each instantiation of the function). The conditioning of the Gallagher function around the global optimum is about 1000.

Contained in the *weakly-structured - weakly-structured* function group.

Links to illustrations of function F_{84} in dimension 5 for the first instance:

- Search space plot along two coordinate axes
- Projection of the search space into a hyperplane through both optima
- Normalized objective space plot (in log-scale)
- Unscaled objective space plot

8.1.85 F_{85}: Schwefel/Katsuuras

Combination of the Schwefel function (f_{20} in the `bbob` suite) and the Katsuuras function (f_{23} in the `bbob` suite).

Both objective functions are highly multi-modal with an exponential number (in the dimension) of (global) optima and only a weak global structure. The most prominent 2^n minima of the Schwefel function are located comparatively close to the corners of the unpenalized search area. The Katsuuras function, in turn, is highly repetitive with more than 10^n global optima.

Links to illustrations of function F_{85} in dimension 5 for the first instance:

- Search space plot along two coordinate axes
- Projection of the search space into a hyperplane through both optima
- Normalized objective space plot (in log-scale)
- Unscaled objective space plot

8.1.86 F_{86}: Schwefel/Lunacek bi-Rastrigin

Combination of the Schwefel function (f_{20} in the `bbob` suite) and the Lunacek bi-Rastrigin function (f_{24} in the `bbob` suite).

Both objective functions are highly multi-modal with only a weak global structure. While the most prominent 2^n minima of the Schwefel function are located comparatively close to the corners of the unpenalized search area, the Lunacek bi-Rastrigin function has two superimposed funnels. Presumably, different approaches need to be used for "selecting the funnel" and for searching the highly multimodal function "within" the funnel. The single-objective Lunacek bi-Rastrigin function was constructed to be deceptive for some evolutionary algorithms with large population size.

Contained in the *weakly-structure - weakly-structured* function group.

Links to illustrations of function F_{86} in dimension 5 for the first instance:

- Search space plot along two coordinate axes
- Projection of the search space into a hyperplane through both optima
- Normalized objective space plot (in log-scale)
- Unscaled objective space plot

8.1.87 F_{87}: Gallagher 101/Gallagher 21

Combination of Gallaghers Gaussian 101-me Peaks function (f_{21} in the `bbob` suite) and the Gallaghers Gaussian 21-hi Peaks function (f_{22} in the `bbob` suite).

Both objective functions are multi-modal and non-separable. Both consist of a set of optima with position and height being unrelated and randomly chosen. The number of optima is 101 and 21 respectively and the condition number around the (unique) global optima are about 30 and about 1000 respectively.

Contained in the *weakly-structured - weakly-structured* function group.

Links to illustrations of function F_{87} in dimension 5 for the first instance:

- Search space plot along two coordinate axes
- Projection of the search space into a hyperplane through both optima
- Normalized objective space plot (in log-scale)
- Unscaled objective space plot

8.1.88 F_{88}: Gallagher 101/Katsuuras

Combination of Gallaghers Gaussian 101-me Peaks function (f_{21} in the `bbob` suite) and the Katsuuras function (f_{23} in the `bbob` suite).

Both objective functions are non-separable and highly multi-modal with only a weak global structure. Gallagher's Gaussian 101-me Peaks function consists of a set of 101 optima with position and height being unrelated and randomly chosen. The conditioning is about 30. The Katsuuras function, in turn, is highly repetitive with more than 10^n global optima.

Contained in the *weakly-structured - weakly-structured* function group.

Links to illustrations of function F_{88} in dimension 5 for the first instance:

- Search space plot along two coordinate axes
- Projection of the search space into a hyperplane through both optima
- Normalized objective space plot (in log-scale)
- Unscaled objective space plot

8.1.89 F_{89}: Gallagher 101/Lunacek bi-Rastrigin

Combination of Gallaghers Gaussian 101-me Peaks function (f_{21} in the `bbob` suite) and the Lunacek bi-Rastrigin function (f_{24} in the `bbob` suite).

Both objective functions are non-separable and highly multi-modal with only a weak global structure. Gallagher's Gaussian 101-me Peaks function consists of a set of 101 optima with position and height being unrelated and randomly chosen. The conditioning is about 30. The Lunacek bi-Rastrigin function has two superimposed funnels. Presumably, different approaches need to be used for "selecting the funnel" and for searching the highly multimodal function "within" the funnel. The single-objective Lunacek bi-Rastrigin function was constructed to be deceptive for some evolutionary algorithms with large population size.

Contained in the *weakly-structured - weakly-structured* function group.

Links to illustrations of function F_{89} in dimension 5 for the first instance:

- Search space plot along two coordinate axes
- Projection of the search space into a hyperplane through both optima
- Normalized objective space plot (in log-scale)
- Unscaled objective space plot

8.1.90 F_{90}: Gallagher 21/Katsuuras

Combination of Gallaghers Gaussian 21-hi Peaks function (f_{22} in the `bbob` suite) and the Katsuuras function (f_{23} in the `bbob` suite).

Both objective functions are non-separable and multi-modal with only a weak global structure. Gallagher's Gaussian 21-hi Peaks function consists of a set of 21 optima with position and height being unrelated and randomly chosen. The conditioning is about 1000. The Katsuuras function, in turn, is highly repetitive with more than 10^n global optima.

Contained in the *weakly-structured - weakly-structured* function group.

Links to illustrations of function F_{90} in dimension 5 for the first instance:

- Search space plot along two coordinate axes
- Projection of the search space into a hyperplane through both optima
- Normalized objective space plot (in log-scale)
- Unscaled objective space plot

8.1.91 F_{91}: Gallagher 21/Lunacek bi-Rastrigin

Combination of Gallaghers Gaussian 21-hi Peaks function (f_{22} in the `bbob` suite) and the Lunacek bi-Rastrigin function (f_{24} in the `bbob` suite).

Both objective functions are non-separable and multi-modal with only a weak global structure. Gallagher's Gaussian 21-hi Peaks function consists of a set of 21 optima with position and height being unrelated and randomly chosen. The conditioning is about 1000. The Lunacek bi-Rastrigin function has two superimposed funnels. Presumably, different approaches need to be used for "selecting the funnel" and for searching the highly multimodal function "within" the funnel. The single-objective Lunacek bi-Rastrigin function was constructed to be deceptive for some evolutionary algorithms with large population size.

Contained in the *weakly-structured - weakly-structured* function group.

Links to illustrations of function F_{91} in dimension 5 for the first instance:

- Search space plot along two coordinate axes
- Projection of the search space into a hyperplane through both optima
- Normalized objective space plot (in log-scale)
- Unscaled objective space plot

8.1.92 F_{92}: Katsuuras/Lunacek bi-Rastrigin

Combination of the Katsuuras function (f_{23} in the `bbob` suite) and the Lunacek bi-Rastrigin function (f_{24} in the `bbob` suite).

Both objective functions are non-separable and highly multi-modal with only a weak global structure. The Katsuuras function is highly repetitive with more than 10^n global optima. The Lunacek bi-Rastrigin function has two superimposed funnels. Presumably, different approaches need to be used for "selecting the funnel" and for searching the highly multimodal function "within" the funnel. The single-objective Lunacek bi-Rastrigin function was constructed to be deceptive for some evolutionary algorithms with large population size.

Contained in the *weakly-structured - weakly-structured* function group.

Links to illustrations of function F_{92} in dimension 5 for the first instance:

- Search space plot along two coordinate axes
- Projection of the search space into a hyperplane through both optima
- Normalized objective space plot (in log-scale)
- Unscaled objective space plot